

Electronic Supplementary Information (ESI)

for

Long-chain aliphatic polyesters from plant oils for injection molding, film extrusion and electrospinning

Florian Stempfle^{†,a}, Benjamin S. Ritter^{†,b,c}, Rolf Mülhaupt^{*,b,c} and Stefan Mecking^{*a}

[†] Both authors contributed equally to this work.

^a Chair of Chemical Materials Science, University of Konstanz, Department of Chemistry, Universitätsstraße 10, 78457 Konstanz, Germany. E-mail: stefan.mecking@uni-konstanz.de; Fax: +49 7531 88-5152; Tel: +49 7531 88-2593

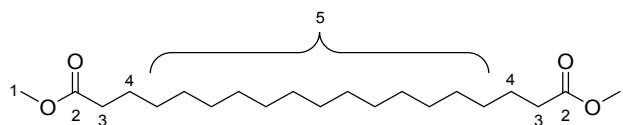
^b Freiburg Materials Research Center (FMF), Stefan-Meier-Straße 21, D-79104 Freiburg, Germany. E-mail: rolf.muelhaupt@makro.uni-freiburg.de; Fax: +49 761 203-6319; Tel: +49 761 203-6273

^c Institute for Macromolecular Chemistry of the University of Freiburg, Stefan-Meier-Straße 31, D-79104 Freiburg, Germany

Table of content

Dimethyl-1,19-nonadecanedioate	S2
Dimethyl-1,23-tricosanedioate	S3
Poly[1,19-nonadecadiyl-1,19-nonadecanedioate] (PE-19.19)	S4
Poly[1,23-tricosadiyl-1,23-tricosanedioate] (PE-23.23)	S5
Rheological properties	S6
Tensile properties	S9
Electrospinning	S10
Dynamic mechanical analysis	S11
Polyester compounds	S12
DMA-analyses of PE-19.19 polymer compound	S13
DSC-analyses of PE-19.19 polymer compound	S18
DMA-analyses of PE-23.23 polymer compound	S23
DSC-analyses of PE-23.23 polymer compound	S28
SEM images of the polymer compounds	S33

Dimethyl-1,19-nonadecanedioate



^1H NMR (CDCl_3 , 25 °C, 400 MHz): δ 3.66 (s, 6H, H-1), 2.30 (t, $^3J_{\text{H-H}} = 7.6$ Hz, 4H, H-3), 1.67-1.56 (m, 4H, H-4), 1.35-1.20 (m, 26H, H-5).

^{13}C NMR (CDCl_3 , 25 °C, 101 MHz): δ 174.48 (s, C-2), 51.56 (s, C-1), 34.28 (s, C-3), 30.16-29.15 (C-5), 25.12 (s, C-4).

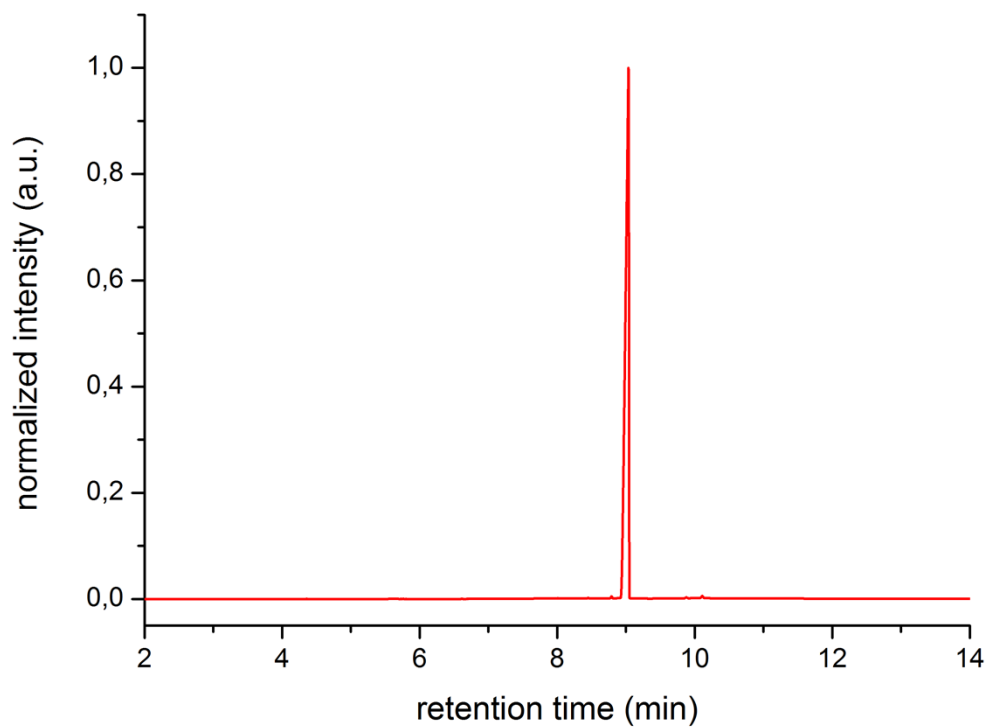
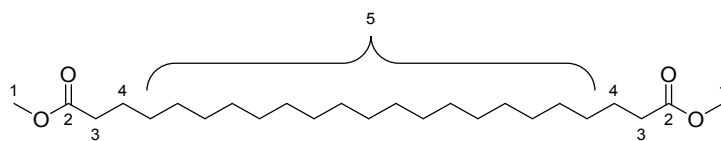


Figure S1: Gas chromatogram (1.0 min isothermal at 90 °C, 30 K min⁻¹ to 280 °C, 8 min) isothermal of pure dimethyl-1,19-nonadecanedioate.

Dimethyl-1,23-tricosanedioate



^1H NMR (CDCl_3 , 25 °C, 400 MHz) δ 3.66 (s, 6H, H-1), 2.29 (t, $^3J_{\text{H-H}} = 7.6$ Hz, 4H, H-3), 1.68-1.58 (m, 4H, H-4), 1.35-1.18 (m, 34H, H-5).

^{13}C NMR (CDCl_3 , 25 °C, 101 MHz): δ 174.45 (s, C-2), 51.55 (s, C-1), 34.27 (s, C-3), 30.18-29.13 (C-5), 25.12 (s, C-4).

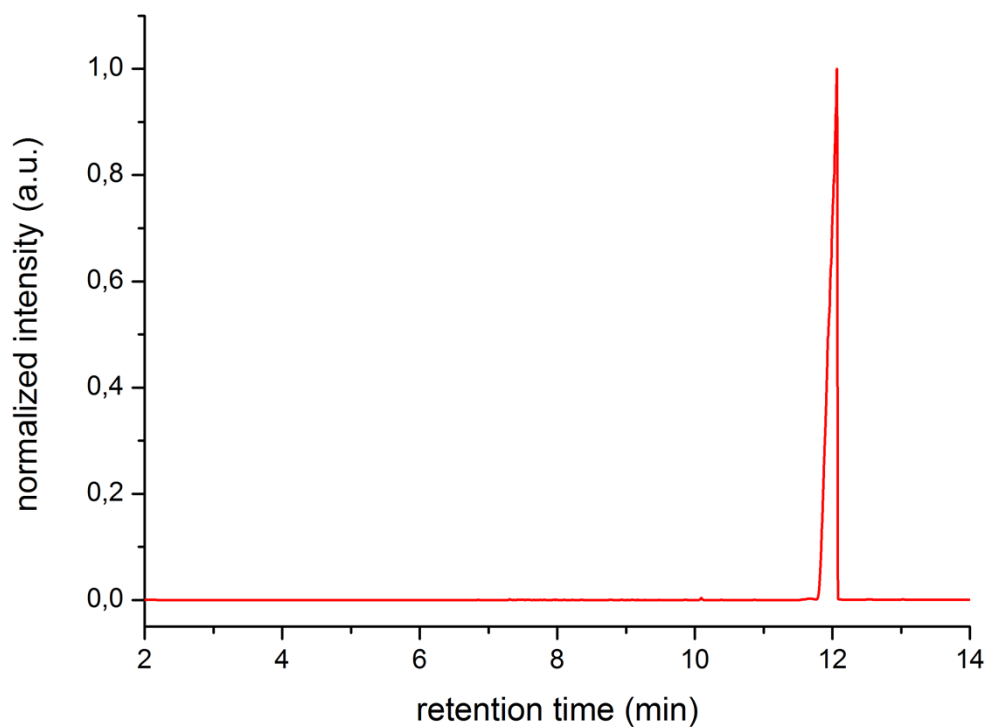


Figure S2: Gas chromatogram (1.0 min isothermal at 90 °C, 30 K min⁻¹ to 280 °C, 8 min) of pure dimethyl-1,23-tricosanedioate.

Poly[1,19-nonadecadiyl-1,19-nonadecanedioate] (PE-19.19)

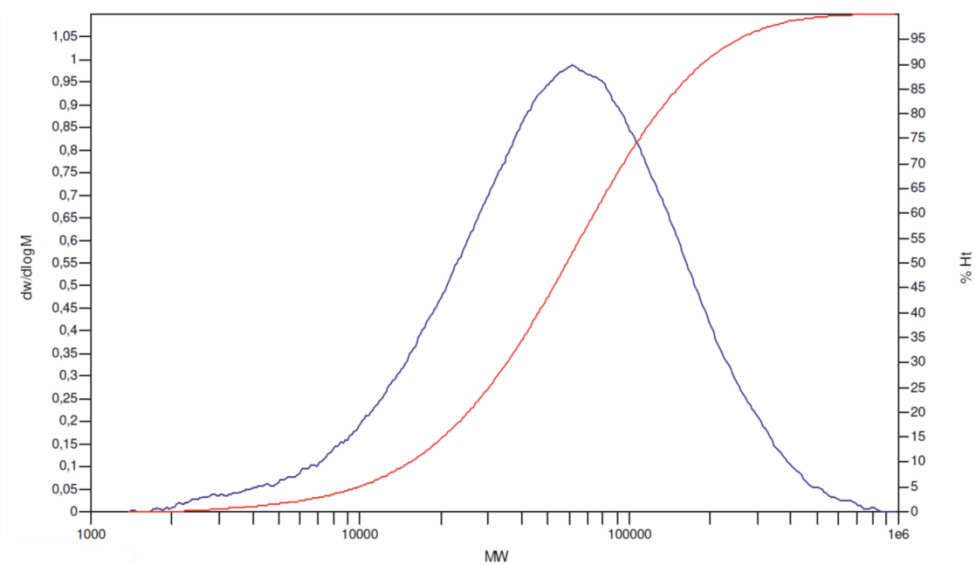


Figure S3: GPC trace (160 °C in 1,2,4-trichlorobenzene, vs. linear polyethylene standards) of PE-19.19.

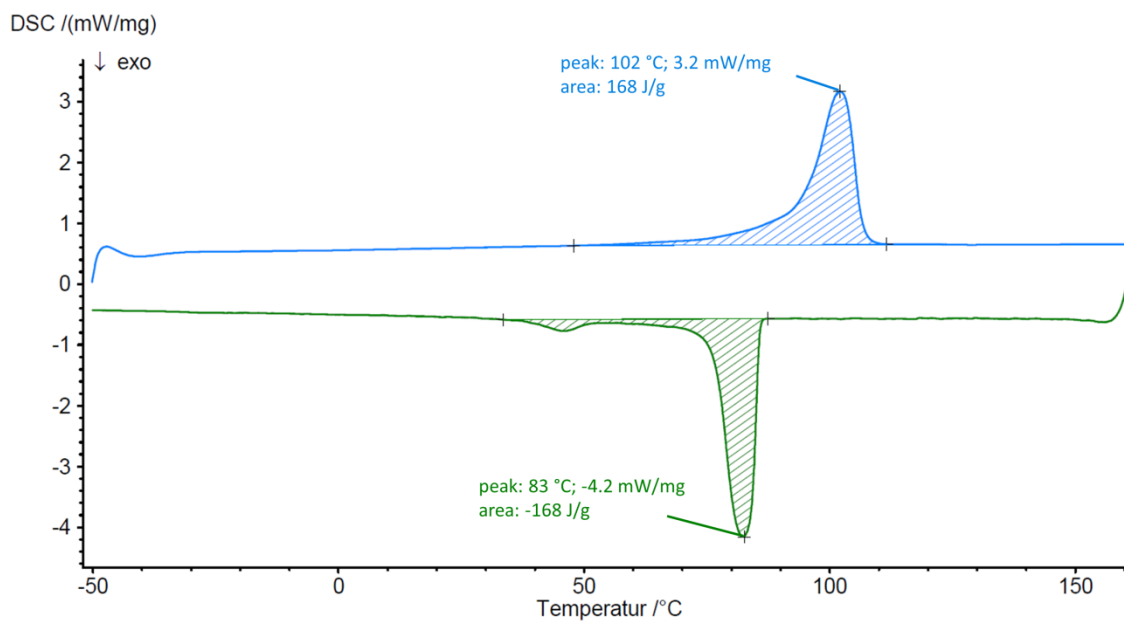


Figure S4: DSC trace (10 K min⁻¹ heating and cooling rate, respectively; data reported are from second heating cycles) of PE-19.19.

Poly[1,23-tricosadiyl-1,23-tricosanedioate] (PE-23.23)

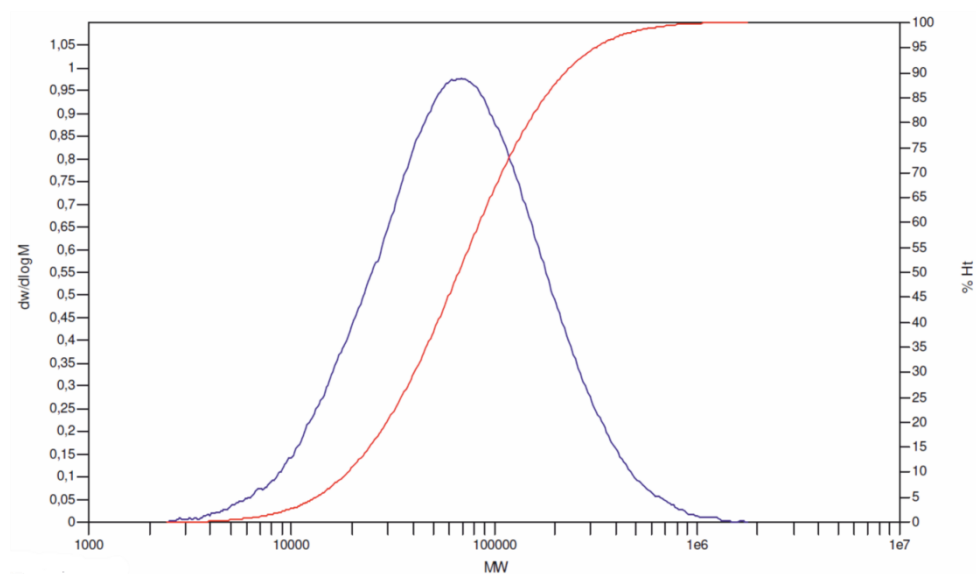


Figure S5: GPC trace (160 °C in 1,2,4-trichlorobenzene, vs. linear polyethylene standards) of PE-23.23.

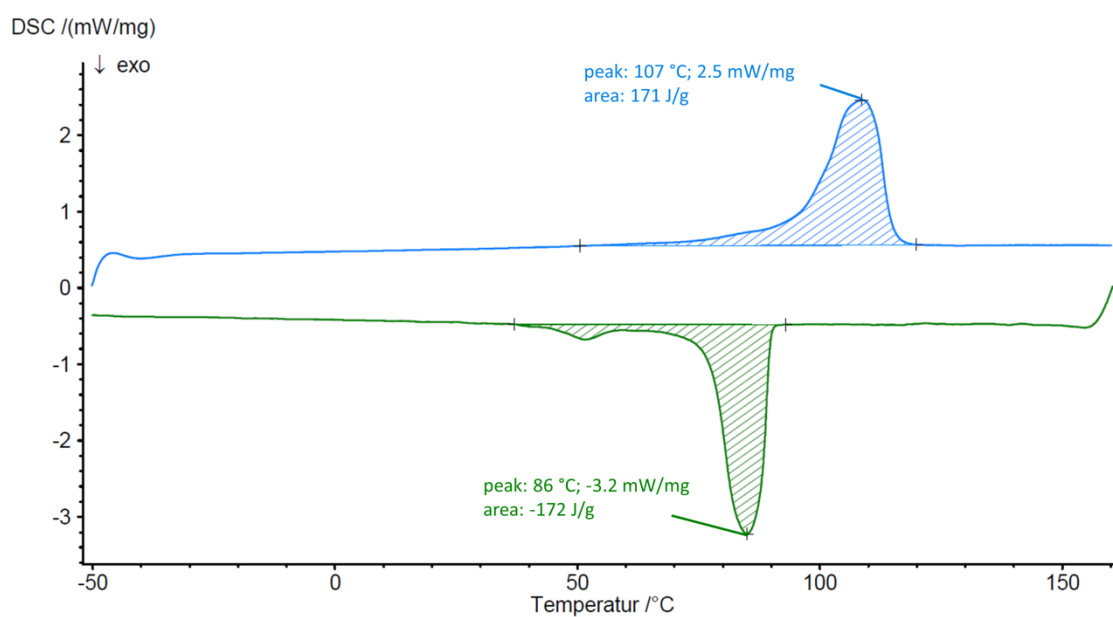


Figure S6: DSC trace (10 K min⁻¹ heating and cooling rate, respectively; data reported are from second heating cycles) of PE-19.19.

Rheological properties

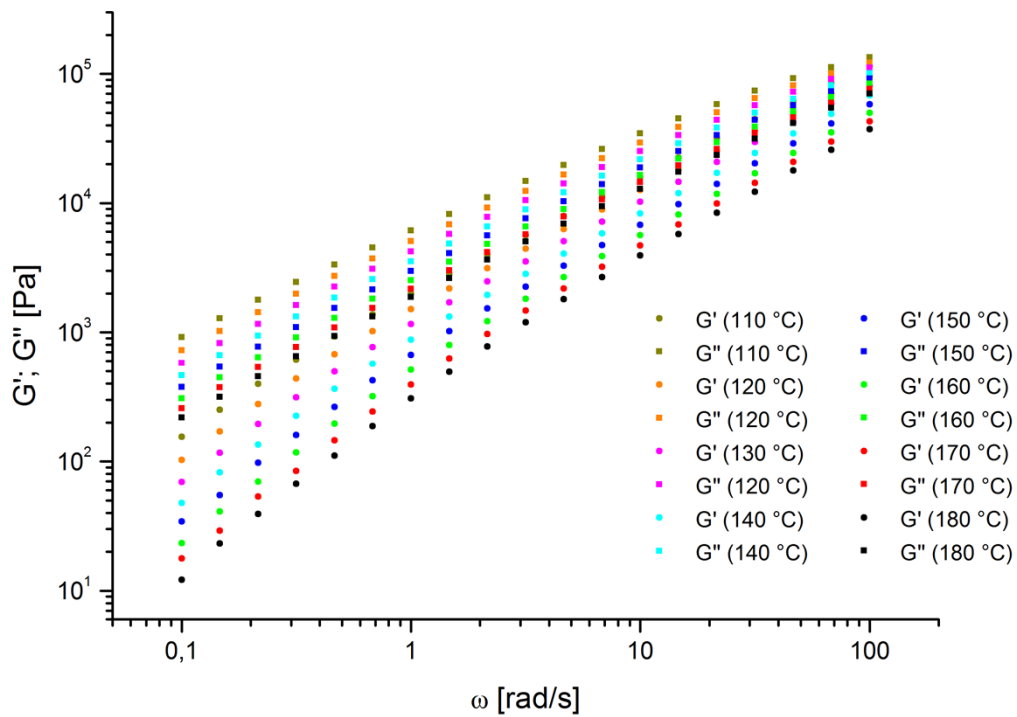


Figure S7: Isothermals of G' and G'' for rheological study of **PE-19.19** (gap = 0.5 mm).

In order to obtain the master curves the isotherms were shifted only in horizontal dimension ($b_T = 1$) at a reference temperature of $T_0 = 150$ °C using the following a_T -values:

Table S1: a_T -values of **PE-19.19**.

entry	temperature [K]	a_T -value
1	383.1	2.727
2	393.1	2.075
3	403.1	1.607
4	413.1	1.266
5	423.1	1.000
6	433.1	0.803
7	443.1	0.655
8	453.1	0.522

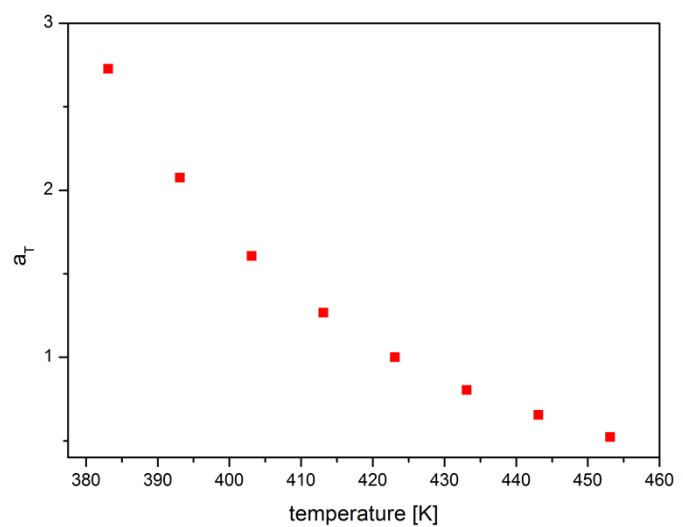


Figure S8: temperature dependence of the a_T -values measured from **PE-19.19**.

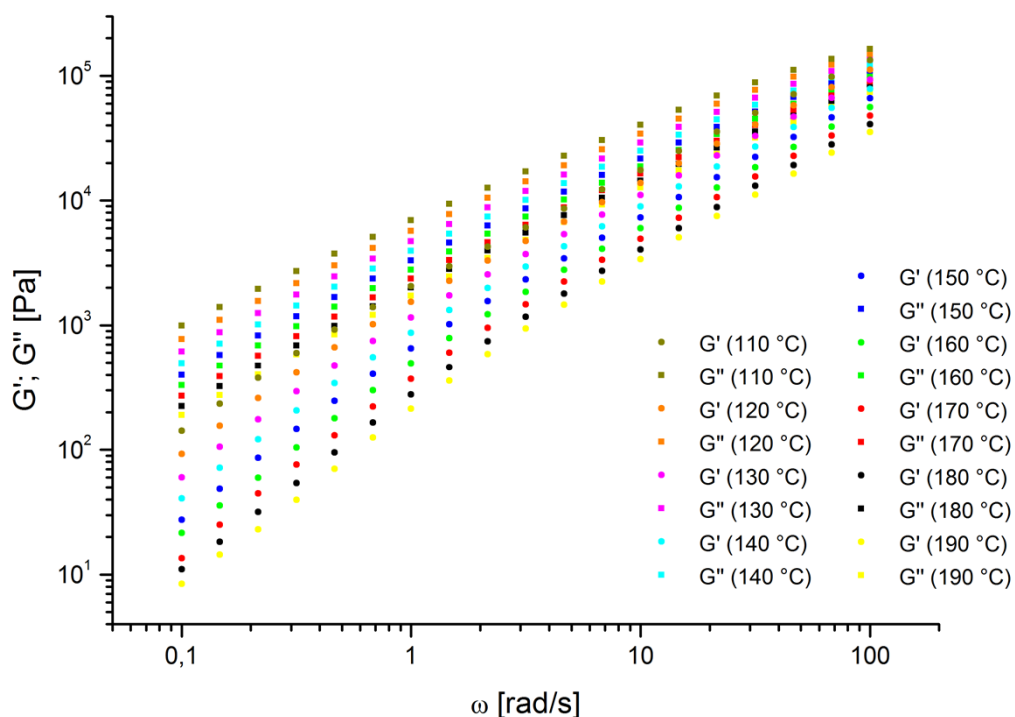


Figure S9: Isothermals of G' and G'' for rheological study of **PE-23.23** (gap = 0.5 mm).

In order to obtain the master curves the isotherms were shifted only in horizontal dimension ($b_T = 1$) at a reference temperature of $T_0 = 150$ °C using the following a_T -values:

Table S2: a_T -values of **PE-23.23**.

entry	temperature [K]	a_T -value
1	383.1	2.650
2	393.1	2.035
3	403.1	1.581
4	413.1	1.251
5	423.1	1.000
6	433.1	0.812
7	443.1	0.660
8	453.1	0.544
9	463.1	0.454

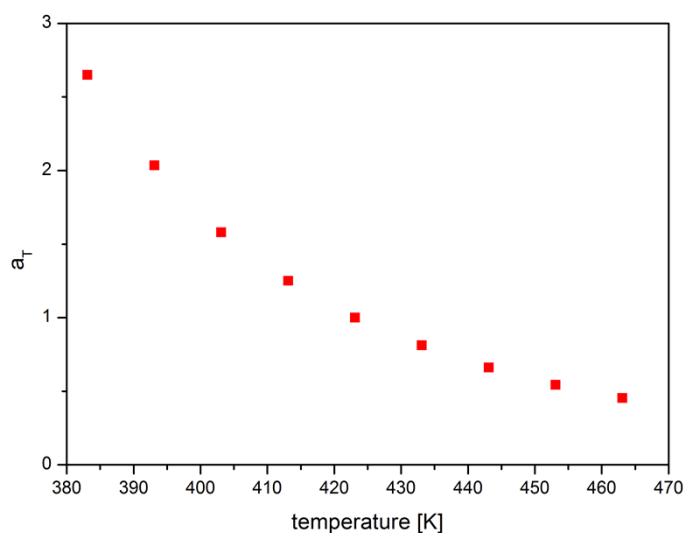


Figure S10: temperature dependence of the a_T -values measured from **PE-23.23**.

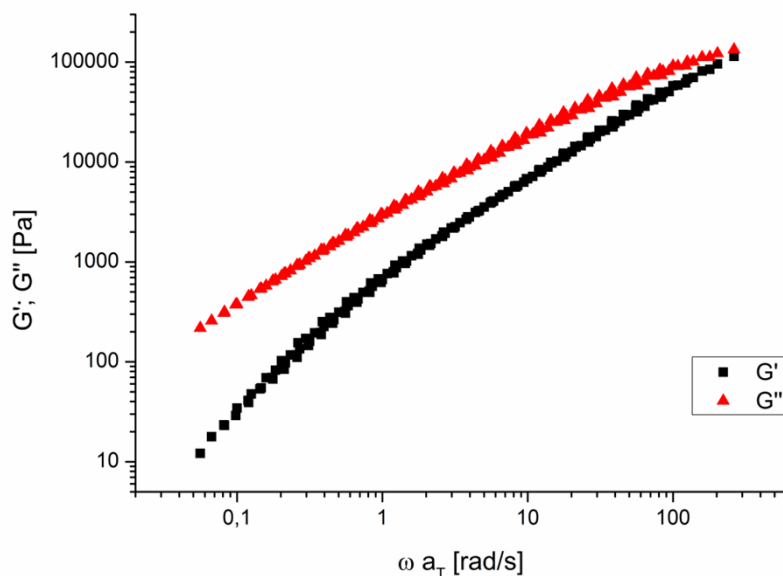


Figure S11: Master curves of G' and G'' for **PE-19.19** (from measurements at 110, 120, 130, 140, 150, 160, 180 and 190 °C). Shifting temperature is 150 °C.

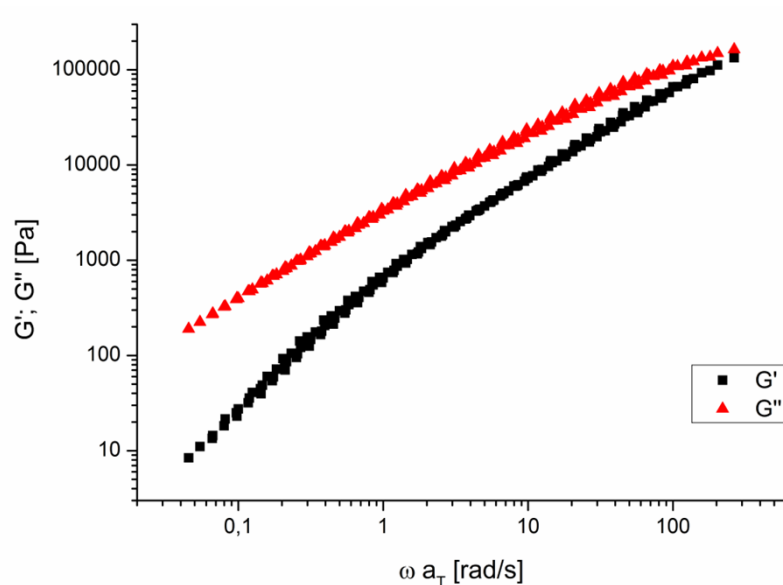


Figure S12: Master curves of G' and G'' for **PE-23.23** (from measurements at 110, 120, 130, 140, 150, 160 and 180 °C). Shifting temperature is 150 °C.

To determine zero-shear viscosity from experimental data, Carreau-Yasuda¹ equation is used:

$$\eta' = \frac{\eta_0}{(1 + a\omega^\alpha)^\beta}$$

Where η' stands for complex viscosity, η_0 is zero-shear viscosity, with ω for frequency and a , α and β are fitting parameters.

The values of parameters in Carreau-Yasuda equation for the studied samples are reported in **Table S3**.

Table S3: Fitted parameters for Carreau-Yasuda equation.

	a	α	β	η_0 [Pa s]
PE-19.19	355	3092	198	3717 \pm 26
PE-23.23	979	3955	1189	4032 \pm 24

Tensile properties

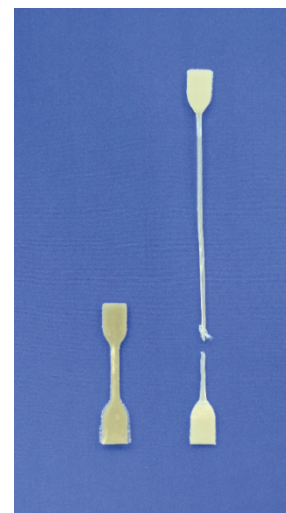
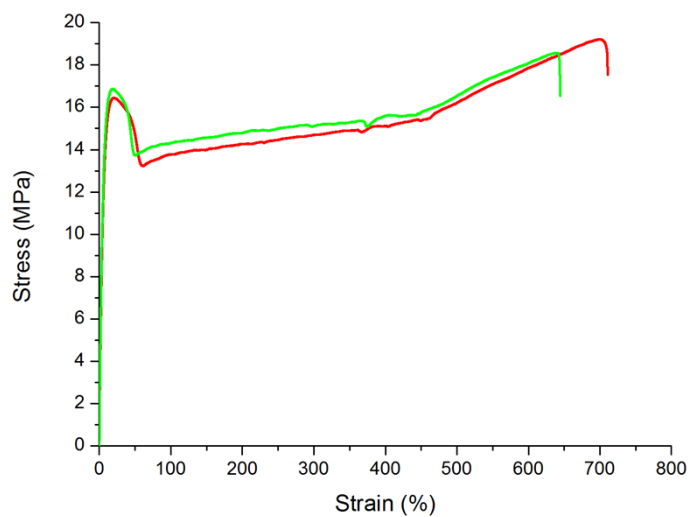


Figure S13: Left: Stress-strain curves (constant drawing rate of 50 mm min⁻¹, room temperature) of **PE-23.23**. Right: Image of test bar for tensile testing before and after strain experiment.

Electrospinning

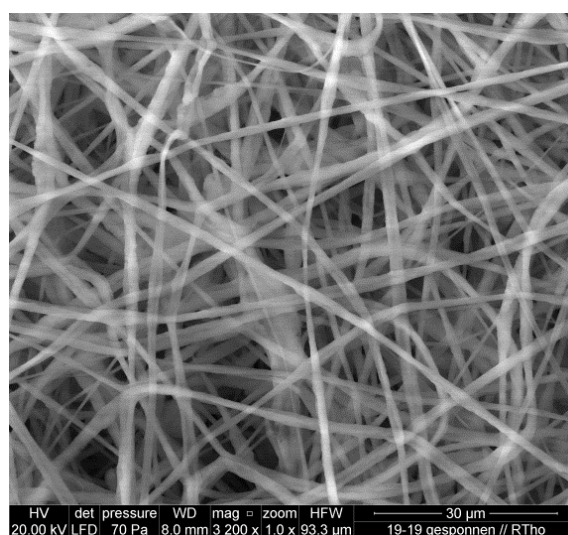
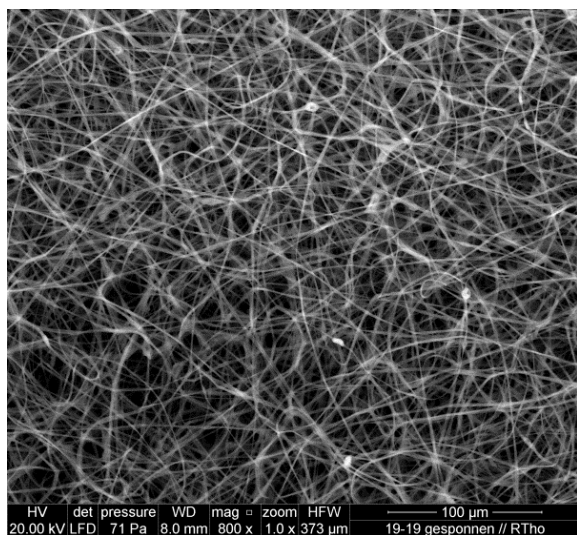


Figure S14: SEM images of electrospun PE19.19 fibers.

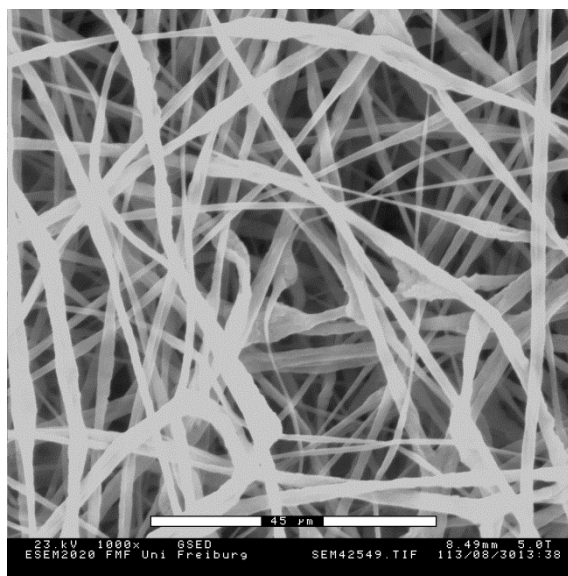
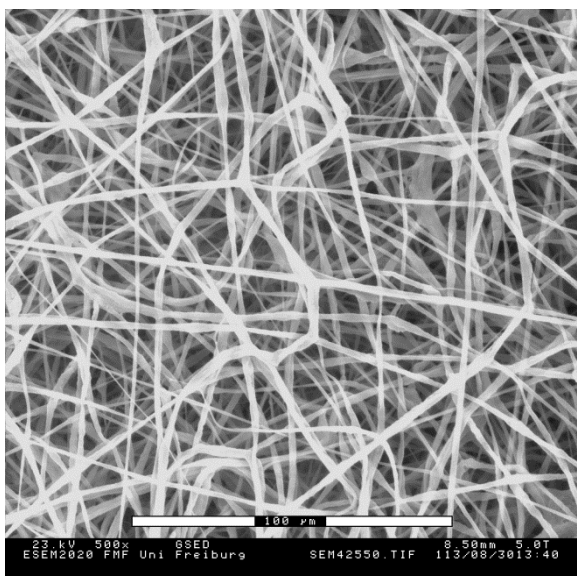


Figure S15: SEM images of electrospun PE23.23 fibers.

Dynamic mechanical analysis

Dynamic mechanical analyses (DMA, at a frequency of 1 Hz) of **PE-23.23** exhibit a glass transition^a around -27 °C; the second relaxation phenomenon at around -130 °C can be ascribed to the motion of the methylene sequences of the polyester main-chain (**Figure S16**).

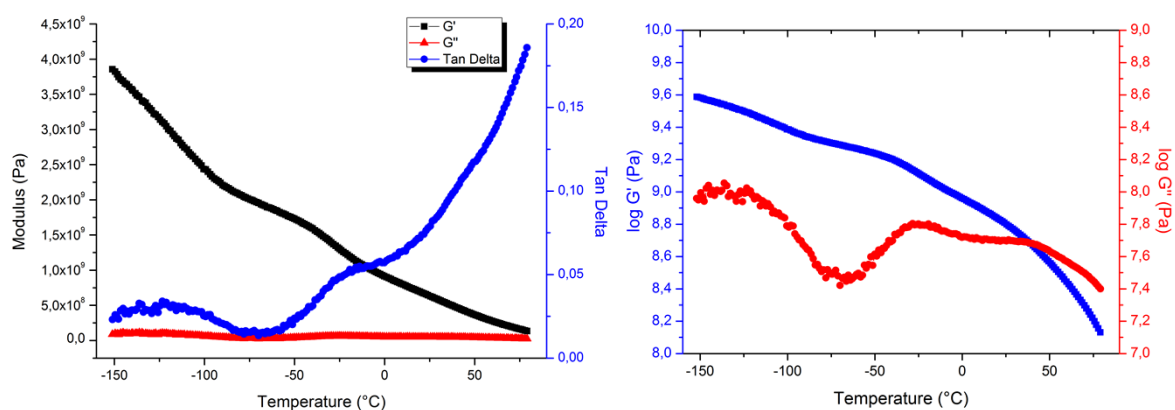


Figure S16: Dynamic mechanical analysis (deformation of 0.1 % and frequency of 1Hz) of **PE-23.23**.

^a Glass transition temperatures (T_g) were determined from maximum in loss modulus (G'').

Polyester compounds

Long-chain polyesters (**PE-19.19** and **PE-23.23**) were blended with various types of commercially available thermoplastics such as linear low density polyethylene (LLDPE, Affinity 8200G) and high density polyethylene (HDPE, Hostalen GC 7260), as well as a thermoplastic elastomer (SEBS, Kraton G1643 MS) and a biodegradable aliphatic-aromatic polyester (Ecoflex F Blend C1200, BASF). Thermal properties of these blends were determined by means of both DMA and DSC measurements. The observation of the thermal transitions of the individual components (and also the moduli) support that the blended polymer combinations studied are not miscible (c.f. **Table S4**).

Table S4: Thermo-mechanical properties of different polymer blends.

	$T_g^a /$ (°C)	$T_g^b /$ (°C)	$T_m^a /$ (°C)	$T_c^a /$ (°C)	$G' (RT)^b /$ (Pa)	$G''(RT)^b /$ (Pa)
PE-19.19 (neat)	-	-37	102	83	1100	84
PE-23.23 (neat)	-	-27	107	86	880	60
Affinity 8200G (neat)	-	-44	65	45	48	2
PE-19.19/Affinity 8200G (15:85 wt.)	-	-45	68/103	44/90	48	2
PE-23.23/Affinity 8200G (15:85 wt.)			66/106	46/90	34	2
Kraton G1643MS (neat)	-39	-36	-	-	38	2
PE-19.19/Kraton G1643MS (15:85 wt.)	-44	-35	100	87	25	2
PE-23.23/Kraton G1643MS (15:85 wt.)	-38		106	54/90	36	3
Ecoflex F Blend C1200 (neat)	-25	-23	124	70	455	25
PE-19.19/Ecoflex F Blend C1200 (15:85 wt.)	-34	-25	102	88	106	6
PE-23.23/Ecoflex F Blend C1200 (15:85 wt.)	-		106	79/92	137	8
Hostalen GC 7260 (neat)	-	-	137	117	1770	130
PE-19.19/Hostalen GC 7260 (15:85 wt.)	-	40	100/134	87/115	1135	113
PE-23.23/Hostalen GC 7260 (15:85 wt.)			106/136	93/116	1470	100

^a Determined by DSC with a heating/cooling rate of 15 K min⁻¹.

^b Determined by DMA (1 Hz, 0.1 % deformation).

DMA-analyses of PE-19.19 polymer compound

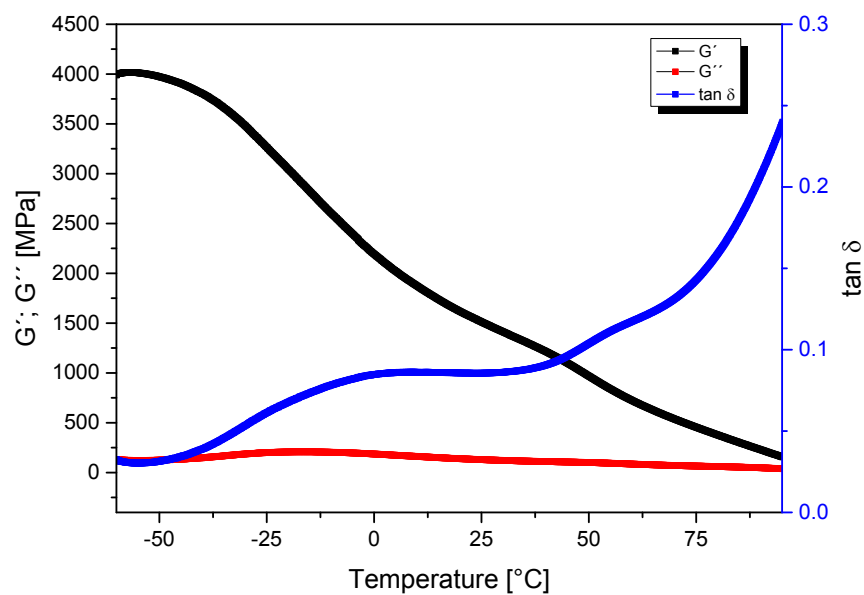


Figure S17: Dynamic mechanical analysis (deformation of 0.1 % and frequency of 1Hz) of PE-19.19 filled with 25 wt.% talc.

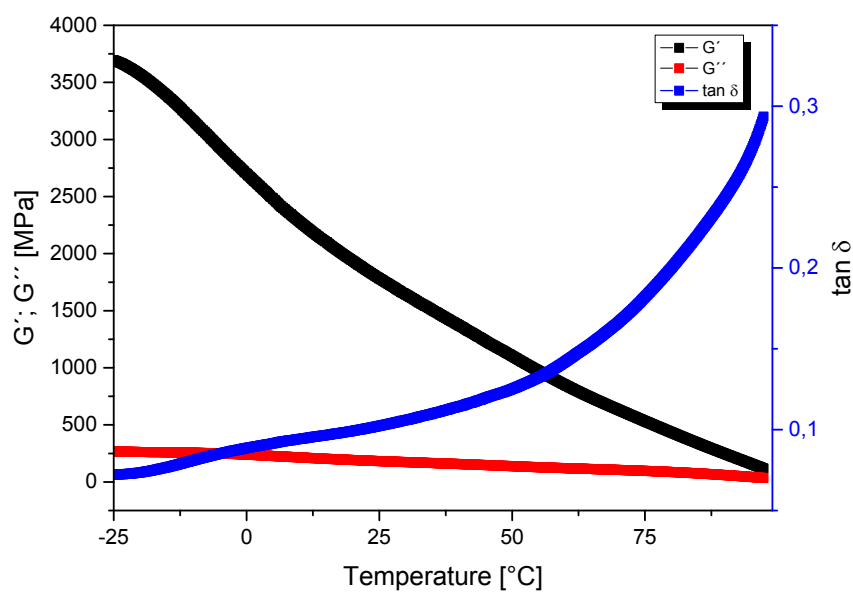


Figure S18: Dynamic mechanical analysis (deformation of 0.1 % and frequency of 1Hz) of PE-19.19 filled with 45 wt.% talc.

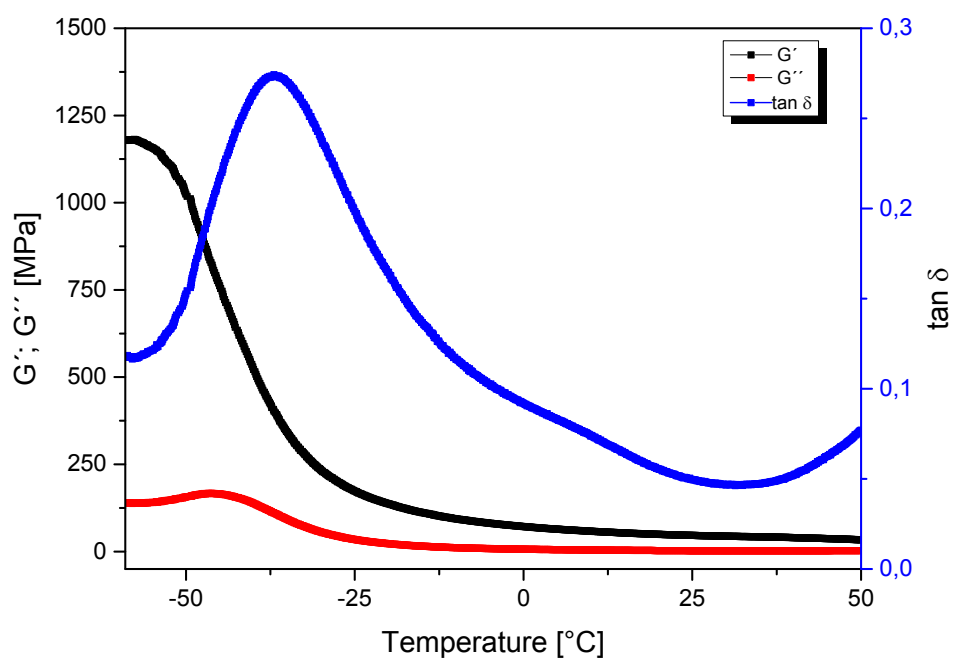


Figure S19: Dynamic mechanical analysis (deformation of 0.1 % and frequency of 1Hz) of 15 wt. % PE-19.19 in Affinity 8200G (LLDPE).

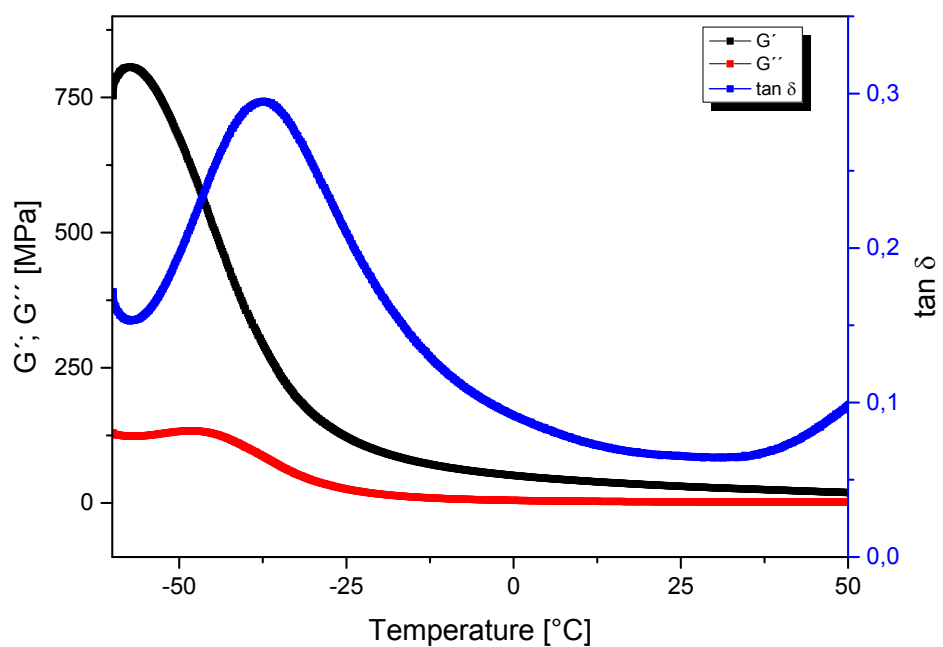


Figure S20: Dynamic mechanical analysis (deformation of 0.1 % and frequency of 1Hz) of 5 wt. % PE-19.19 in Affinity 8200G (LLDPE).

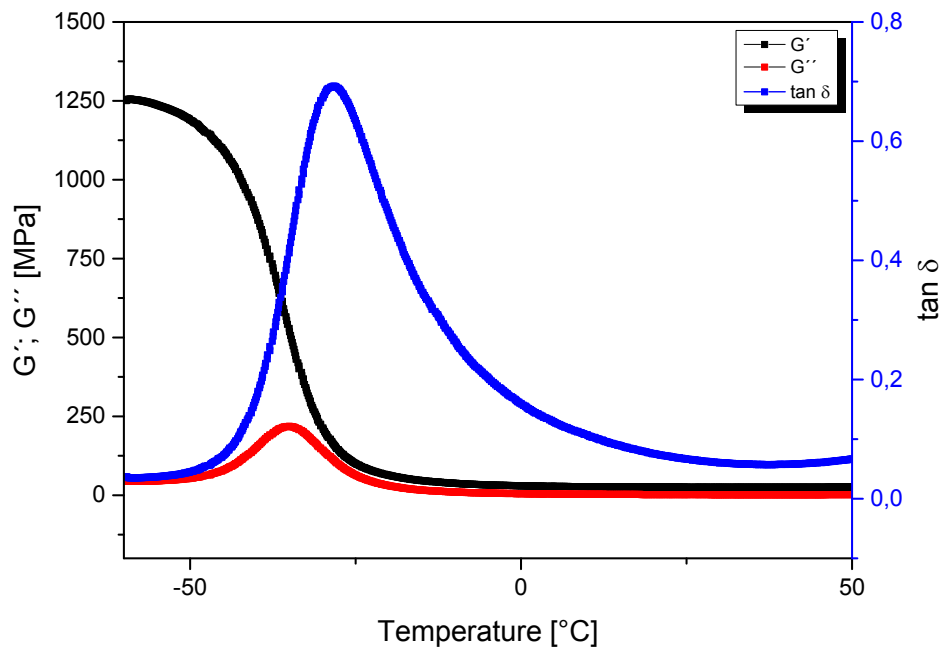


Figure S21: Dynamic mechanical analysis (deformation of 0.1 % and frequency of 1Hz) of 15 wt. % PE-19.19 in Kraton G1643 MS (SEBS).

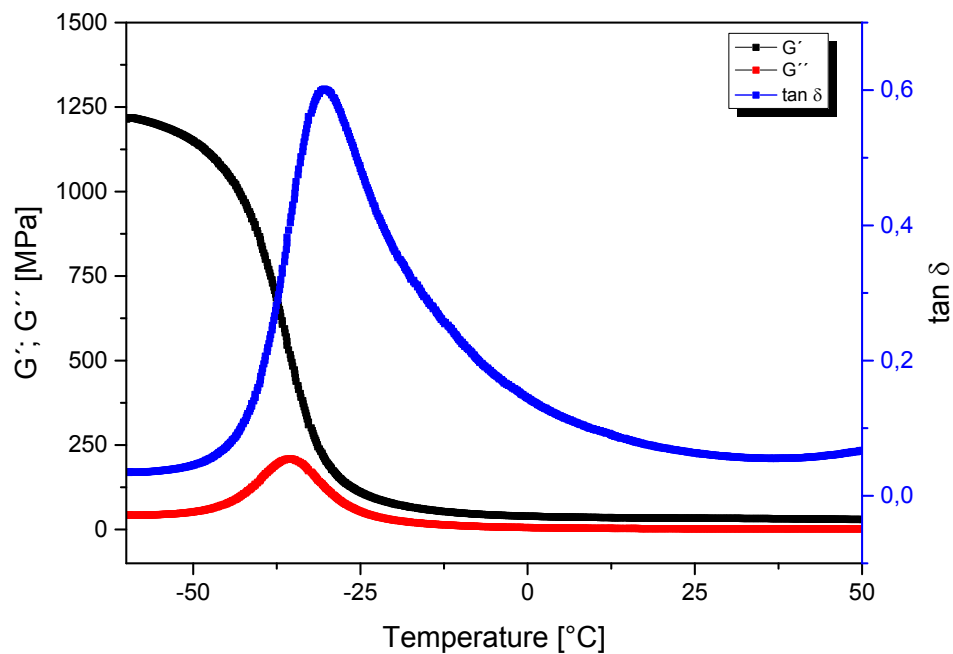


Figure S22: Dynamic mechanical analysis (deformation of 0.1 % and frequency of 1Hz) of 5 wt. % PE-19.19 in Kraton G1643 MS (SEBS).

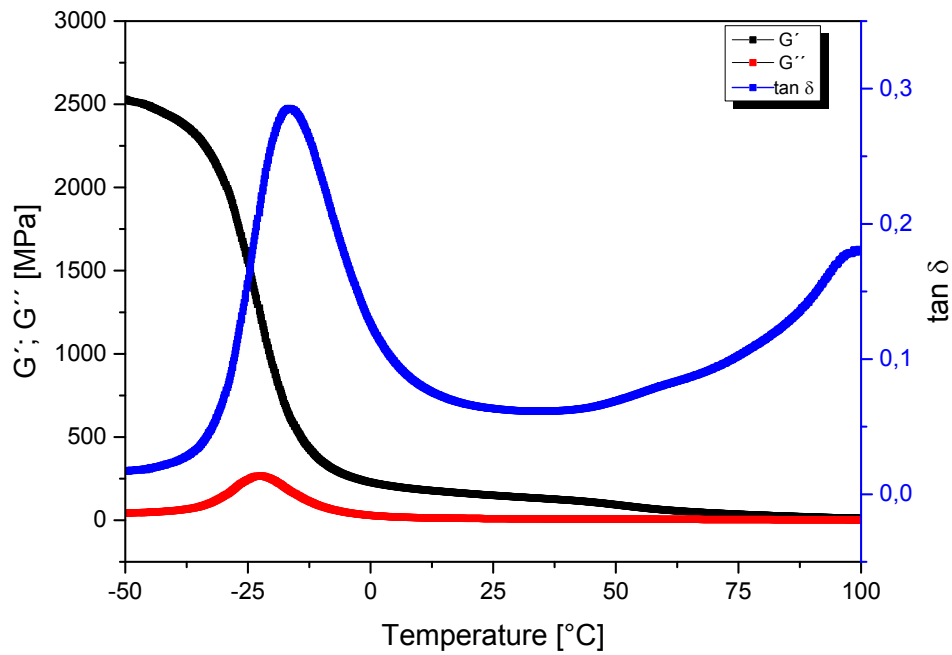


Figure S23: Dynamic mechanical analysis (deformation of 0.1 % and frequency of 1Hz) of 15 wt. % PE-19.19 in Ecoflex F Blend C1200.

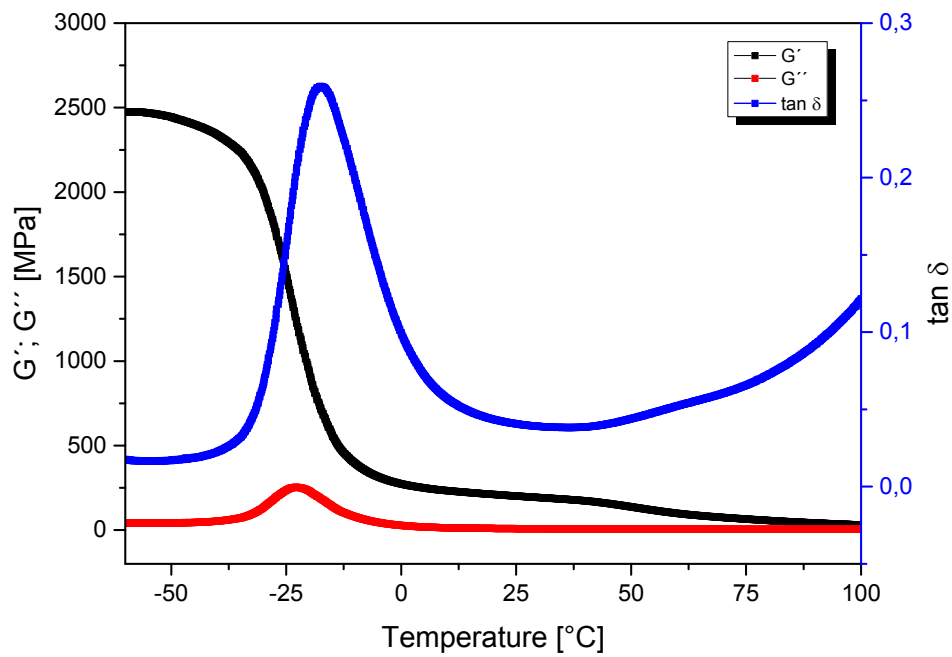


Figure S24: Dynamic mechanical analysis (deformation of 0.1 % and frequency of 1Hz) of 5 wt. % PE-19.19 in Ecoflex F Blend C1200.

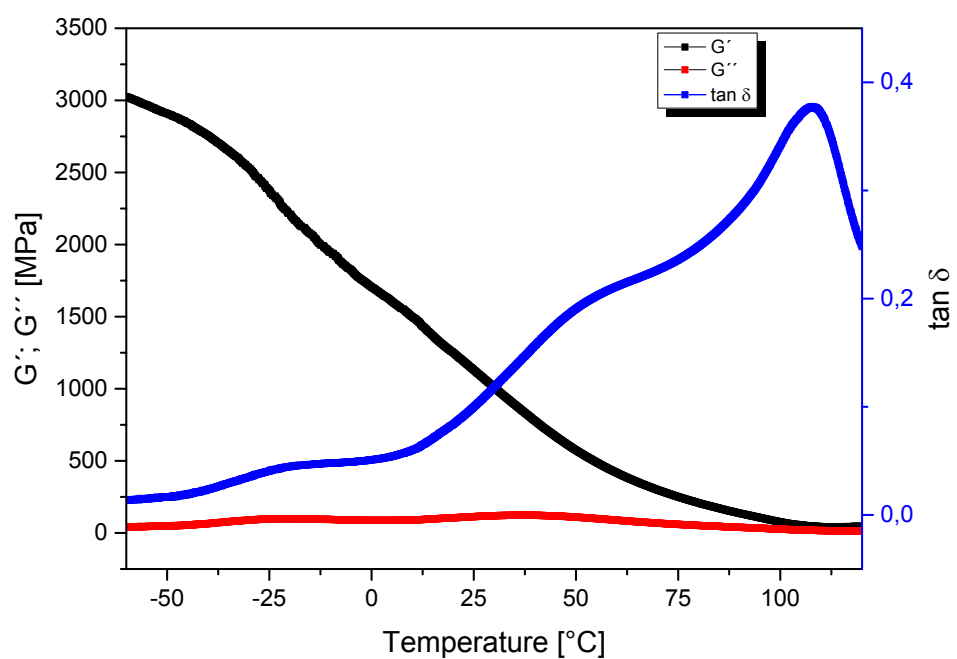


Figure S25: Dynamic mechanical analysis (deformation of 0.1 % and frequency of 1Hz) of 25 wt. % **PE-19.19** in Hostalen GC 7260 (HDPE).

DSC-analyses of PE-19.19 polymer compound

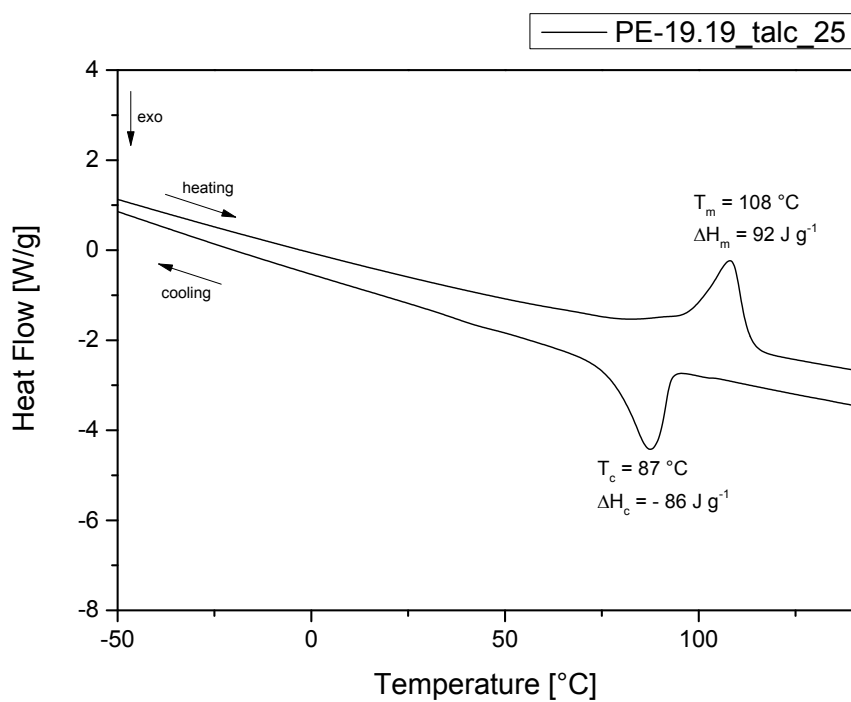


Figure S26: DSC analysis (15 K min^{-1} heating and cooling rate, respectively; data reported are from second heating cycles) of PE-19.19 filled with 25 wt.% talc.

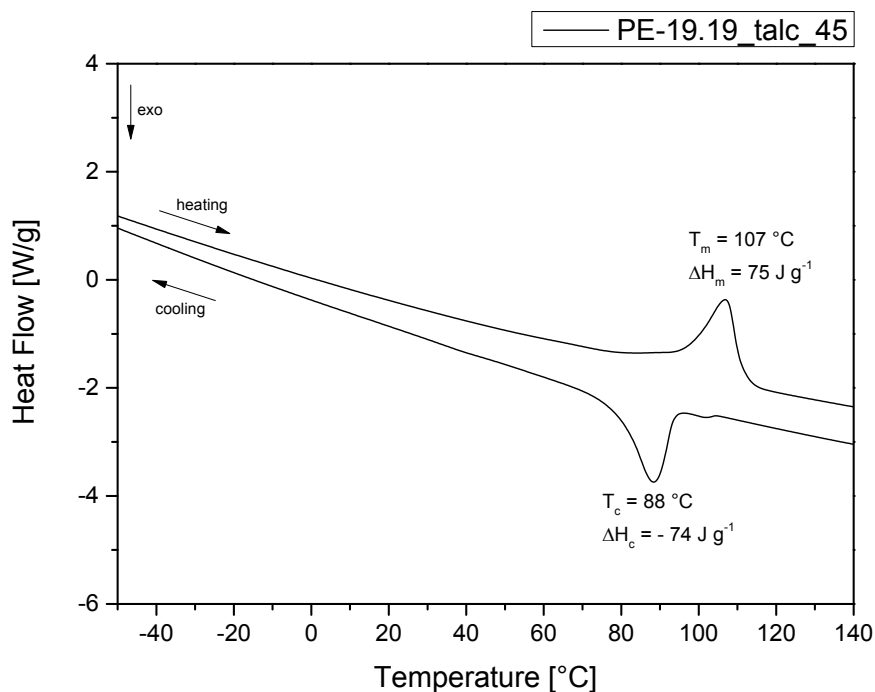


Figure S27: DSC analysis (15 K min^{-1} heating and cooling rate, respectively; data reported are from second heating cycles) of PE-19.19 filled with 45 wt.% talc.

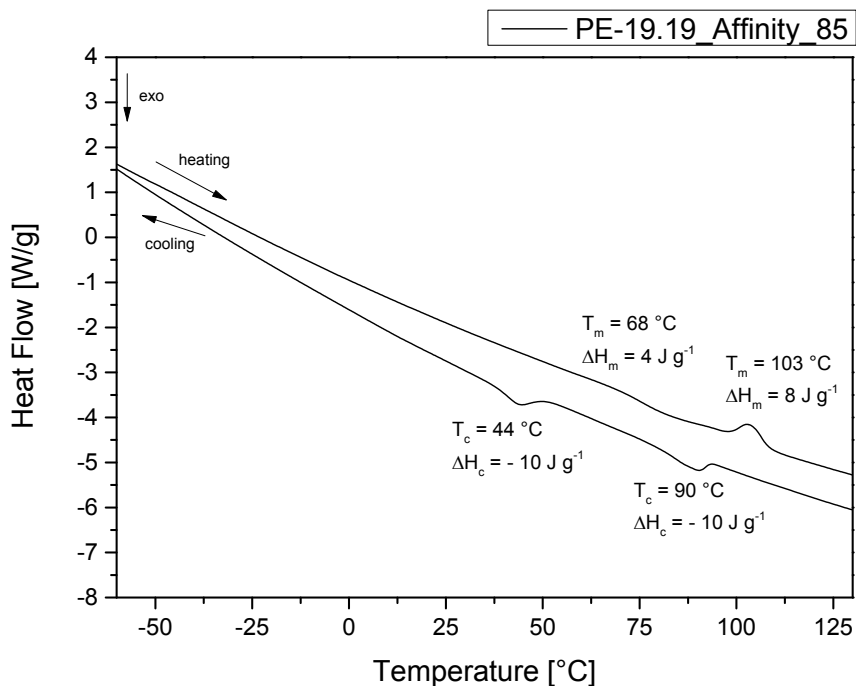


Figure S28: DSC analysis (15 K min^{-1} heating and cooling rate, respectively; data reported are from second heating cycles) of 15 wt. % PE-19.19 in Affinity 8200G (LLDPE).

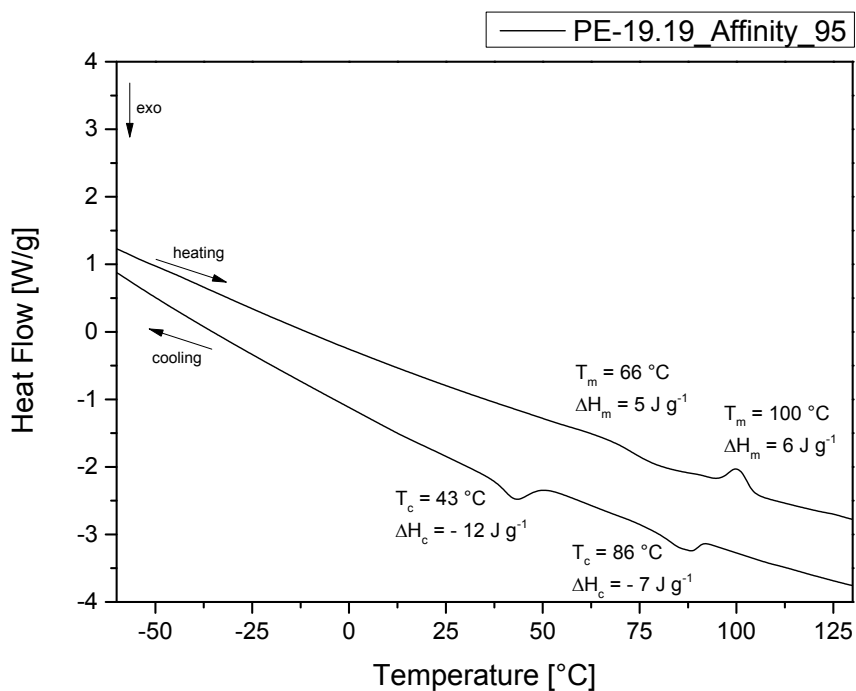


Figure S29: DSC analysis (15 K min^{-1} heating and cooling rate, respectively; data reported are from second heating cycles) of 5 wt. % PE-19.19 in Affinity 8200G (LLDPE).

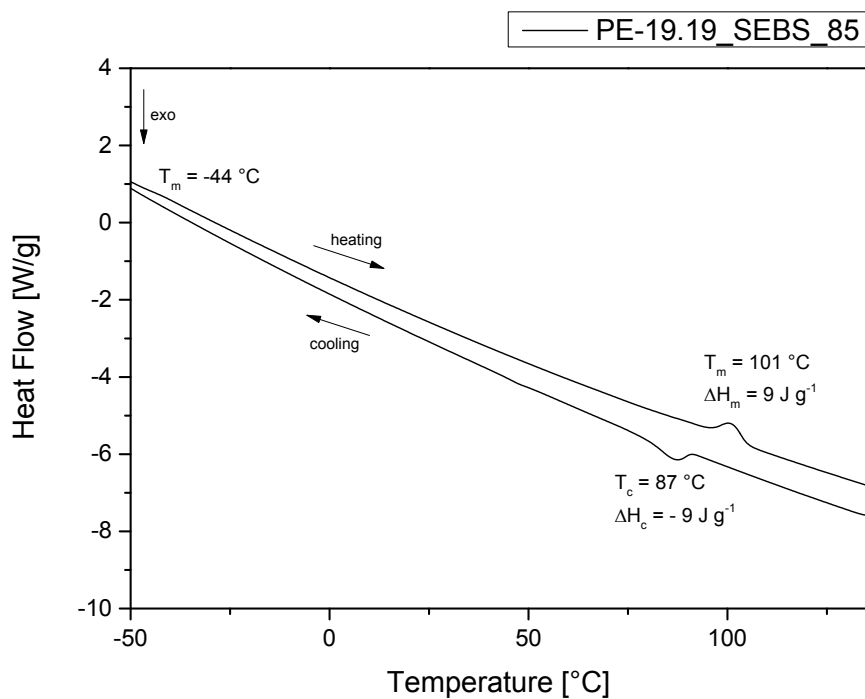


Figure S30: DSC analysis (15 K min^{-1} heating and cooling rate, respectively; data reported are from second heating cycles) of 15 wt. % PE-19.19 in Kraton G1643 MS (SEBS).

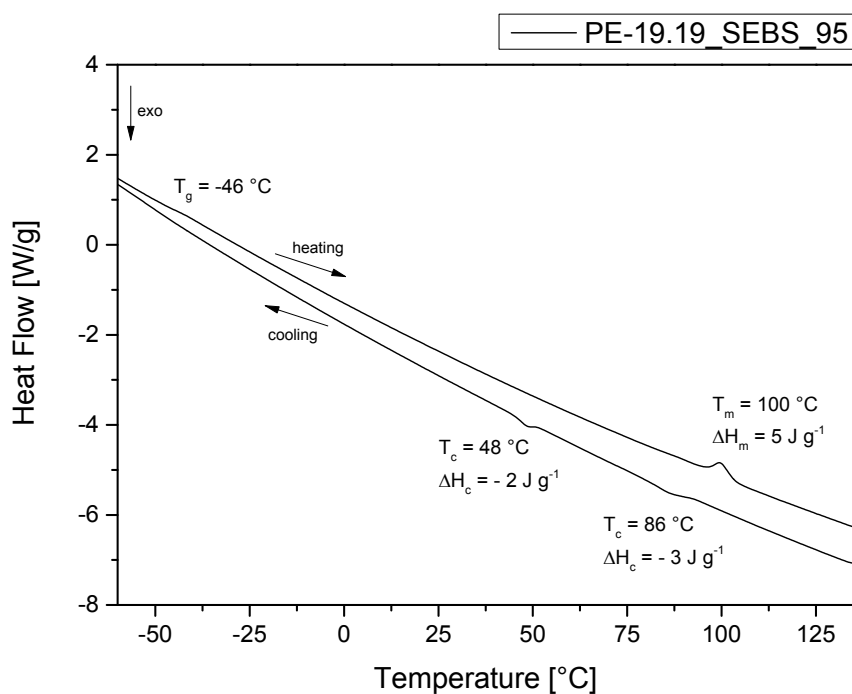


Figure S31: DSC analysis (15 K min^{-1} heating and cooling rate, respectively; data reported are from second heating cycles) of 5 wt. % PE-19.19 in Kraton G1643 MS (SEBS).

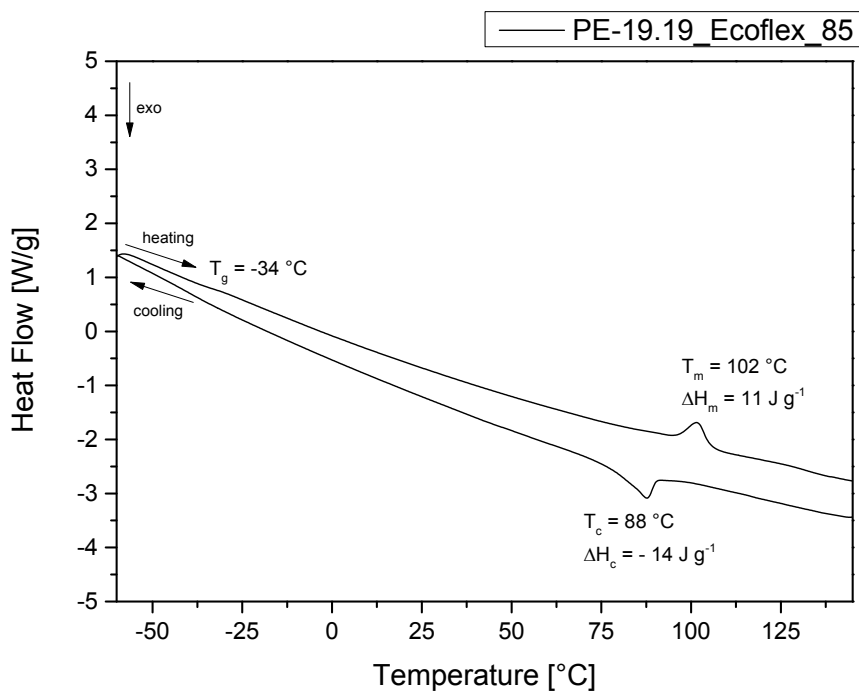


Figure S32: DSC analysis (15 K min^{-1} heating and cooling rate, respectively; data reported are from second heating cycles) of 15 wt. % PE-19.19 in Ecoflex.

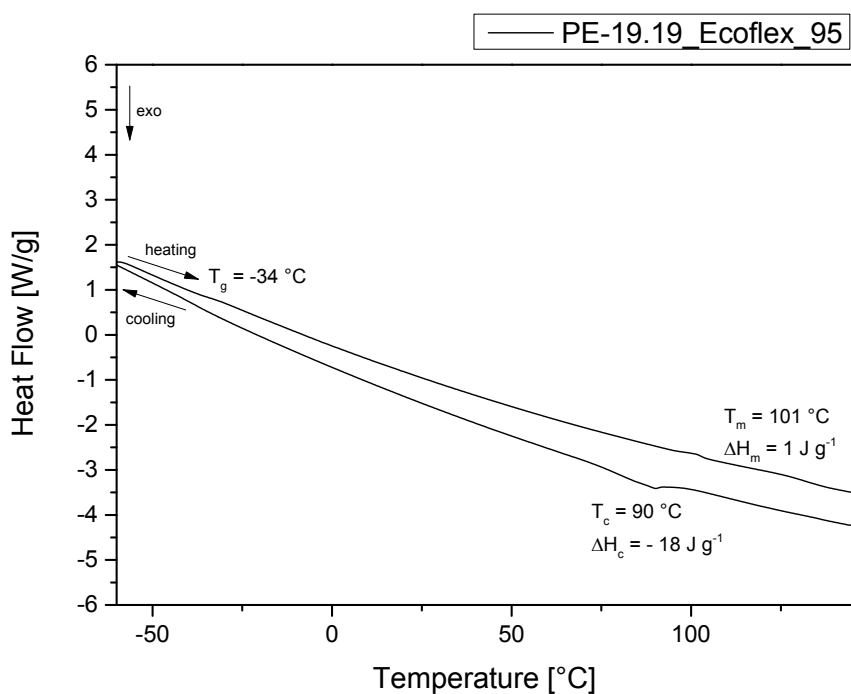


Figure S33: DSC analysis (15 K min^{-1} heating and cooling rate, respectively; data reported are from second heating cycles) of 5 wt. % PE-19.19 in Ecoflex F Blend C1200.

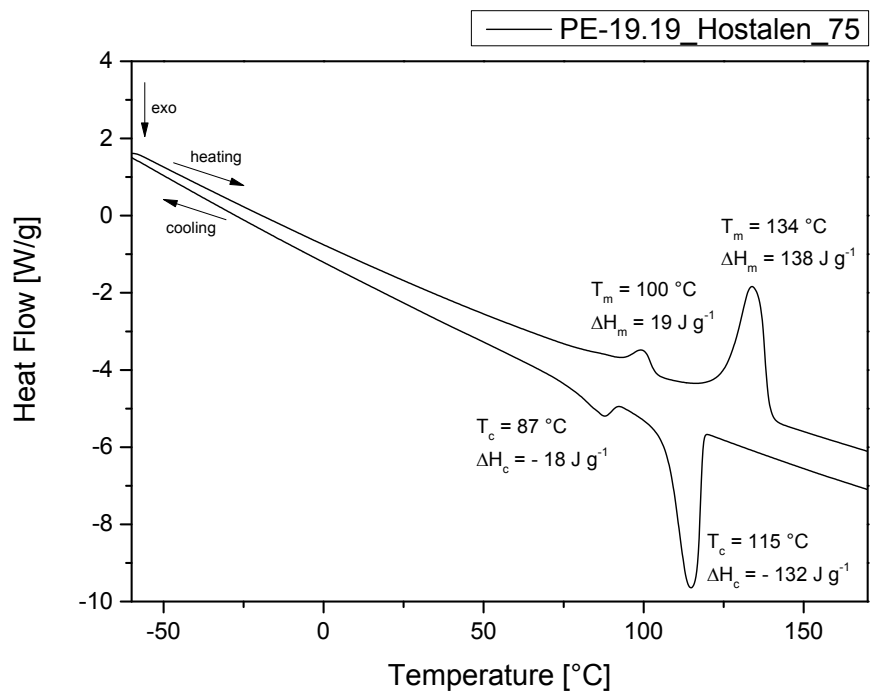


Figure S34: DSC analysis (15 K min^{-1} heating and cooling rate, respectively; data reported are from second heating cycles) of 25 wt. % PE-19.19 in Hostalen GC 7260 (HDPE).

DMA-analyses of PE-23.23 polymer compounds

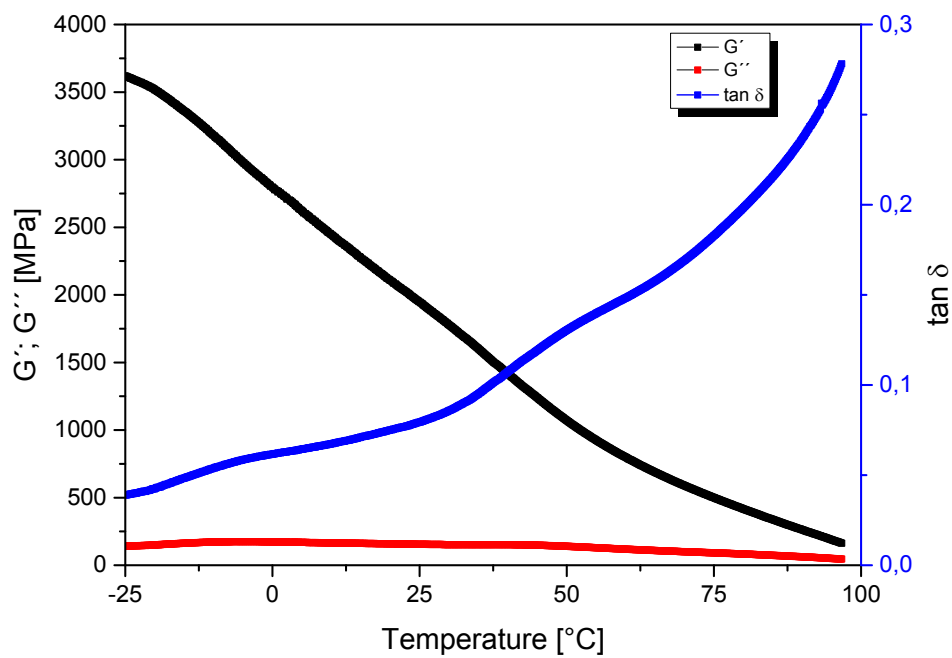


Figure S35: Dynamic mechanical analysis (deformation of 0.1 % and frequency of 1Hz) of PE-23.23 filled with 25 wt.% talc.

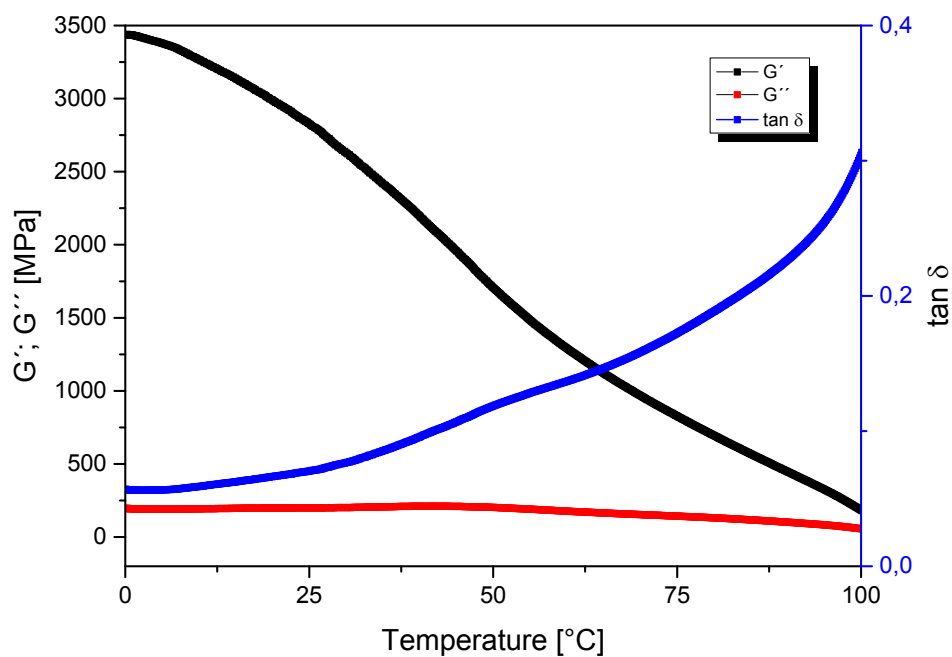


Figure S36: Dynamic mechanical analysis (deformation of 0.1 % and frequency of 1Hz) of PE-23.23 filled with 45 wt.% talc.

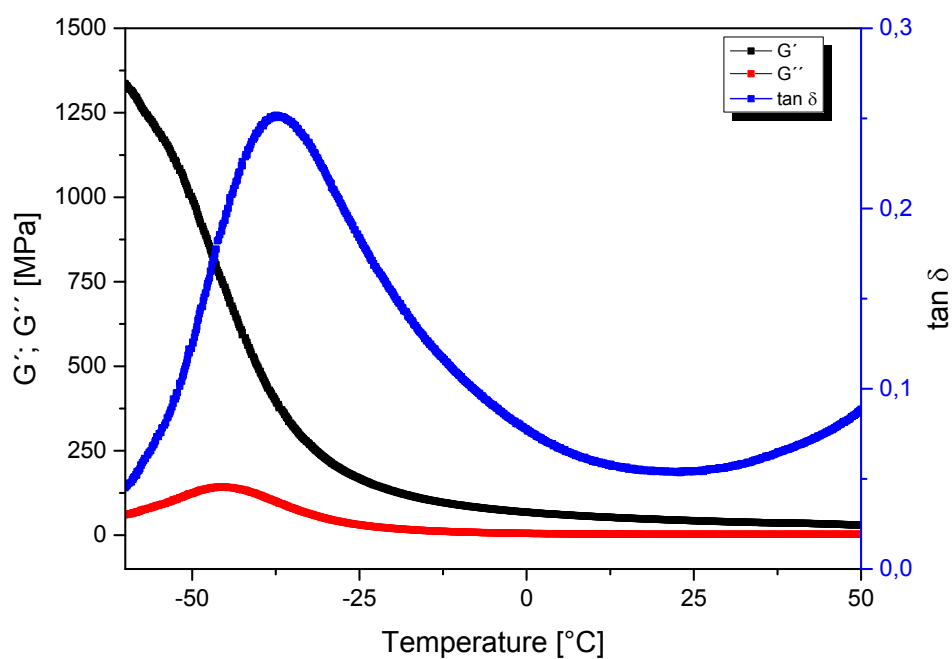


Figure S37: Dynamic mechanical analysis (deformation of 0.1 % and frequency of 1Hz) of 15 wt. % PE-23.23 in Affinity 8200G (LLDPE).

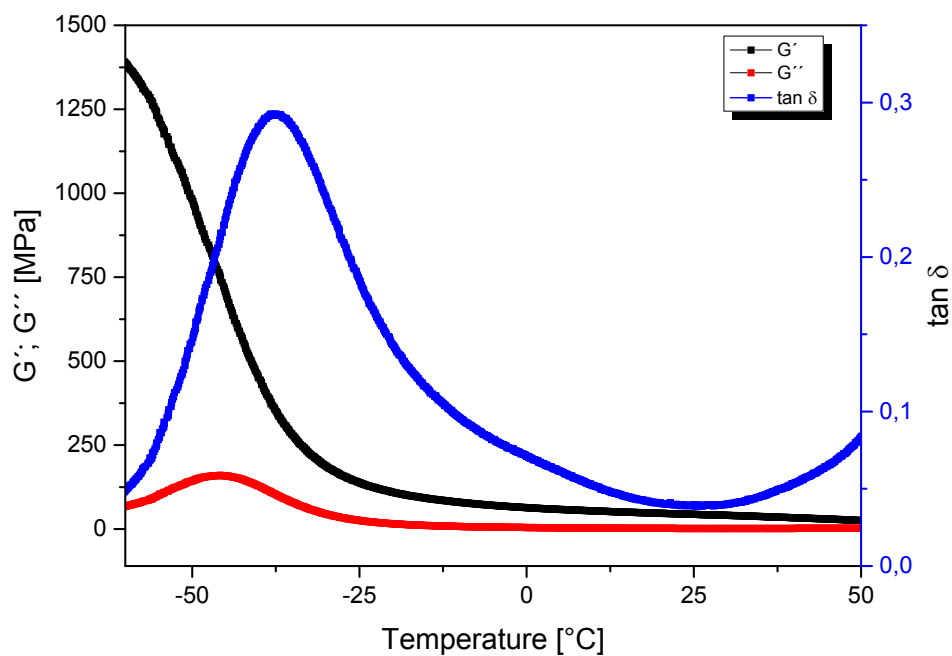


Figure S38: Dynamic mechanical analysis (deformation of 0.1 % and frequency of 1Hz) of 5 wt. % PE-23.23 in Affinity 8200G (LLDPE).

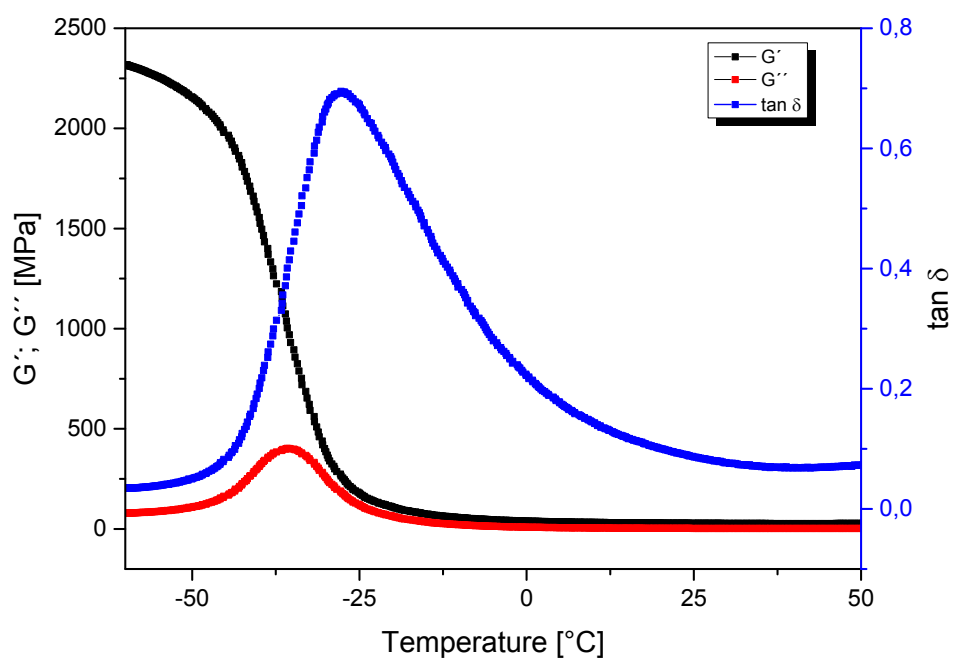


Figure S39: Dynamic mechanical analysis (deformation of 0.1 % and frequency of 1Hz) of 15 wt. % PE-23.23 in Kraton G1643 MS (SEBS).

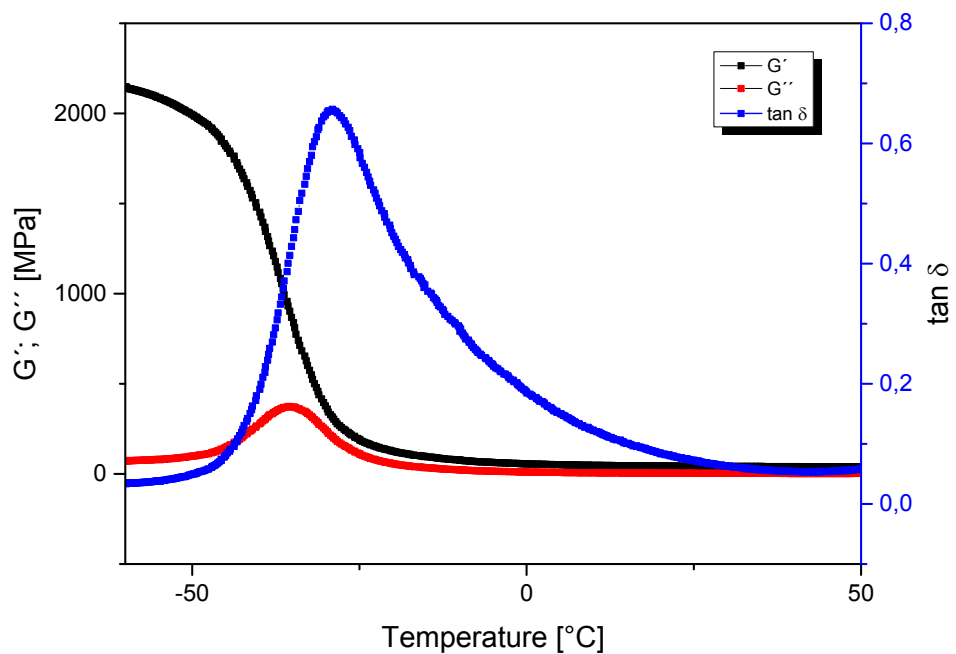


Figure S40: Dynamic mechanical analysis (deformation of 0.1 % and frequency of 1Hz) of 5 wt. % PE-23.23 in Kraton G1643 MS (SEBS).

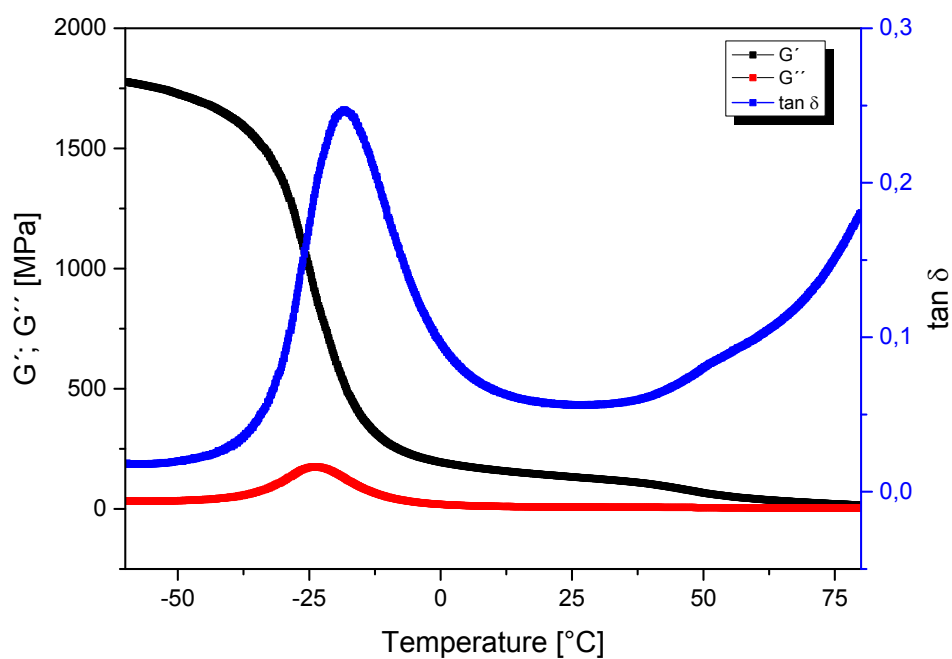


Figure S41: Dynamic mechanical analysis (deformation of 0.1 % and frequency of 1Hz) of 15 wt. % PE-23.23 in Ecoflex F Blend C1200.

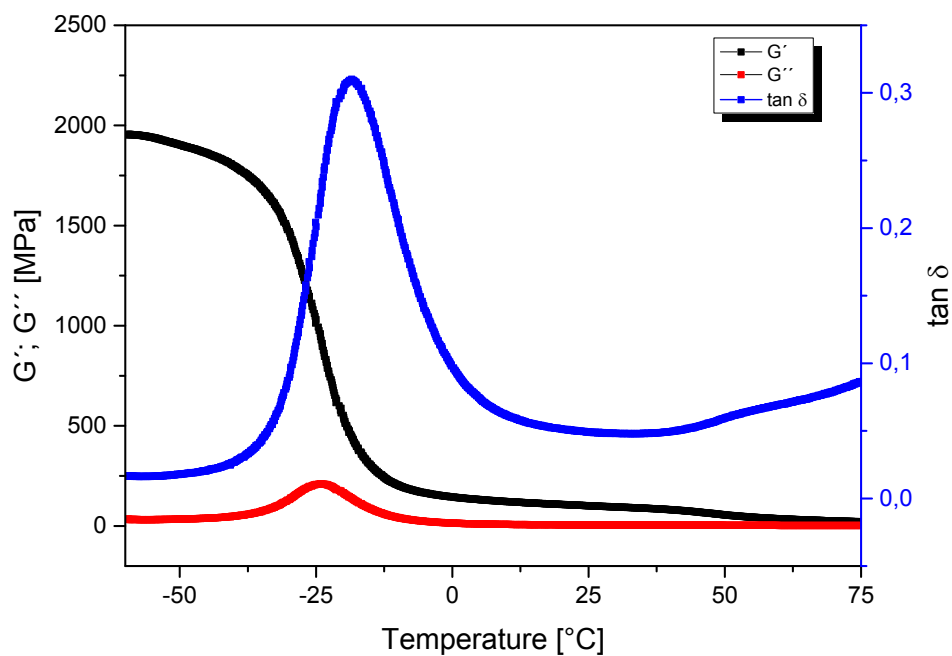


Figure S42: Dynamic mechanical analysis (deformation of 0.1 % and frequency of 1Hz) of 5 wt. % PE-23.23 in Ecoflex F Blend C1200.

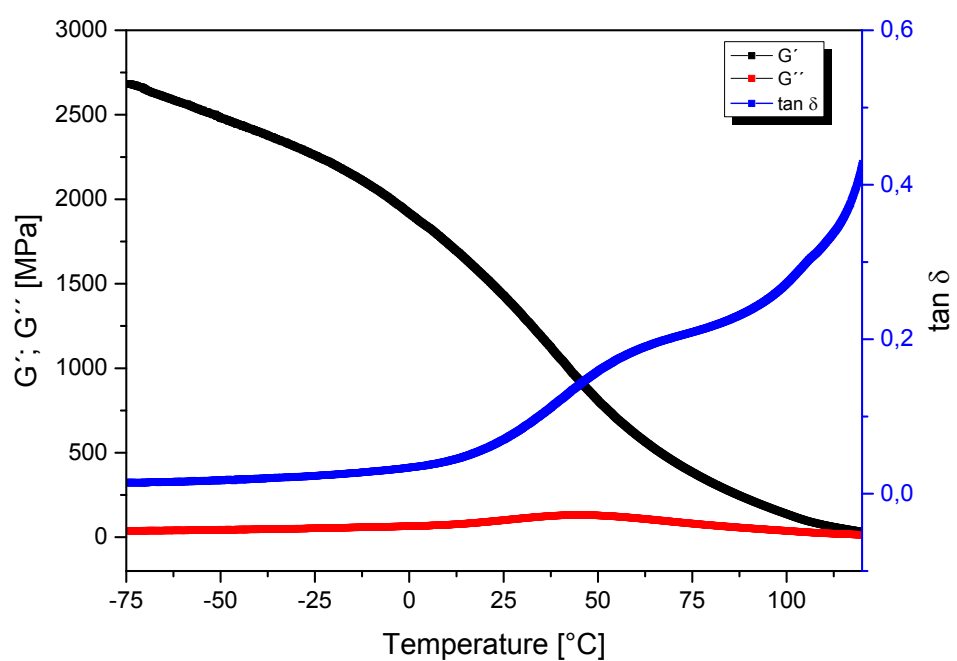


Figure S43: Dynamic mechanical analysis (deformation of 0.1 % and frequency of 1Hz) of 15 wt. % **PE-23.23** in Hostalen GC 7260 (HDPE).

DSC-analyses of PE-23.23 polymer compound

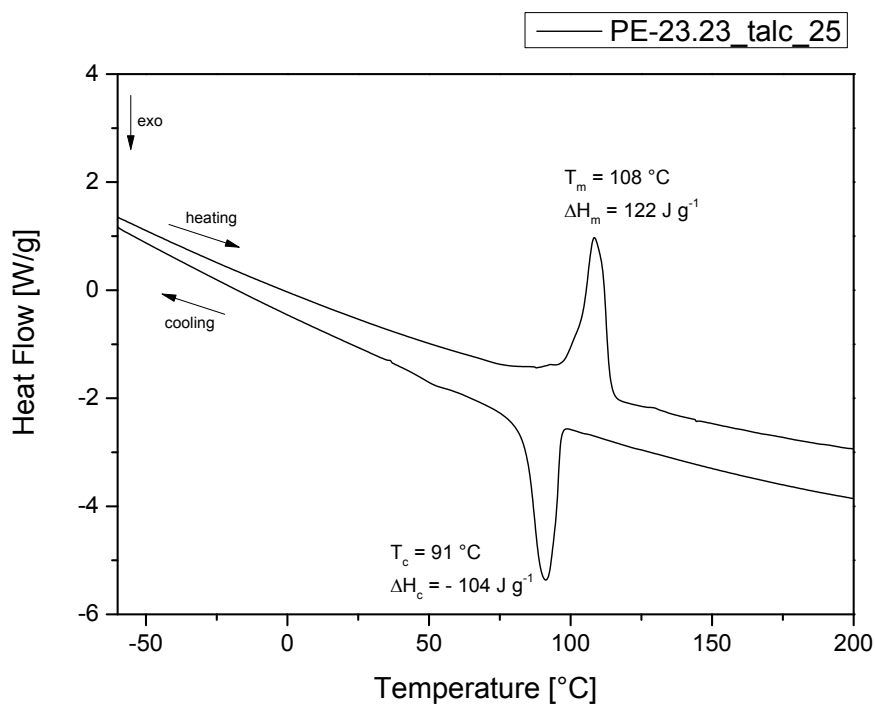


Figure S44: DSC analysis (15 K min^{-1} heating and cooling rate, respectively; data reported are from second heating cycles) of PE-23.23 filled with 25 wt.% talc.

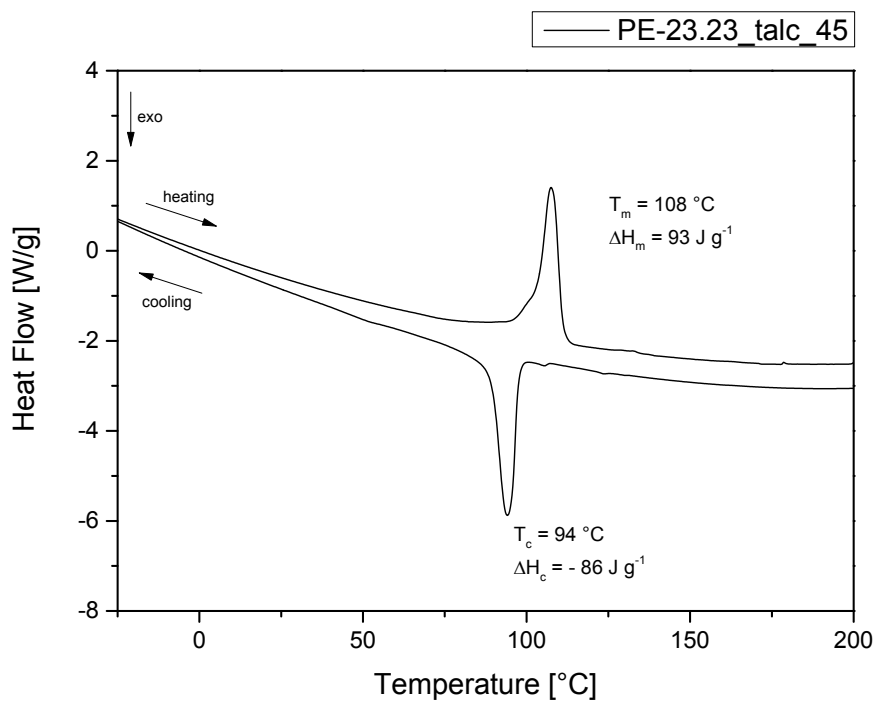


Figure S45: DSC analysis (15 K min^{-1} heating and cooling rate, respectively; data reported are from second heating cycles) of PE-23.23 filled with 45 wt.% talc.

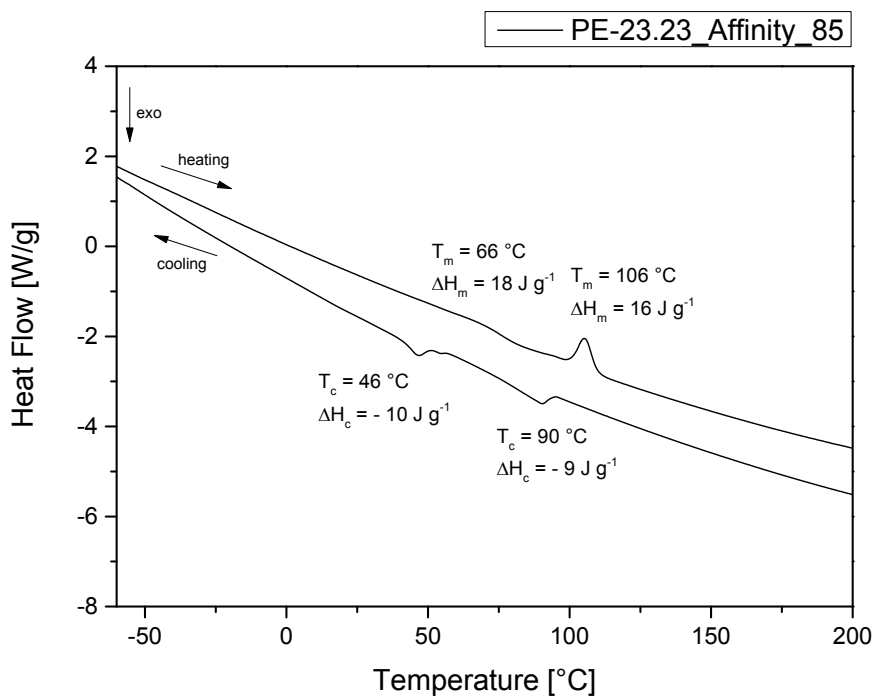


Figure S46: DSC analysis (15 K min^{-1} heating and cooling rate, respectively; data reported are from second heating cycles) of 15 wt. % PE-23.23 in Affinity 8200G (LLDPE).

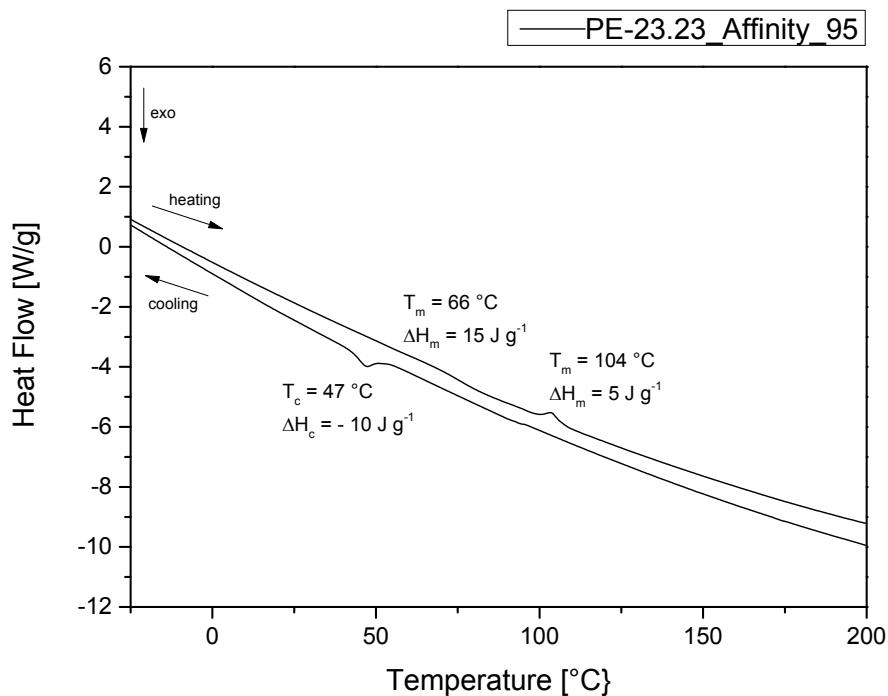


Figure S47: DSC analysis (15 K min^{-1} heating and cooling rate, respectively; data reported are from second heating cycles) of 5 wt. % PE-23.23 in Affinity 8200G (LLDPE).

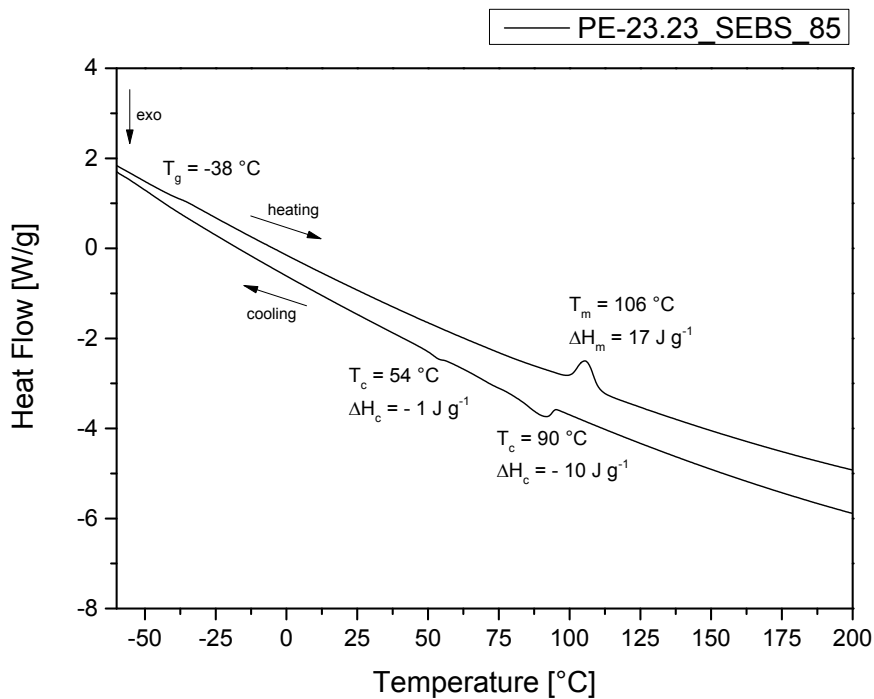


Figure S48: DSC analysis (15 K min^{-1} heating and cooling rate, respectively; data reported are from second heating cycles) of 15 wt. % PE-23.23 in Kraton G1643 MS (SEBS).

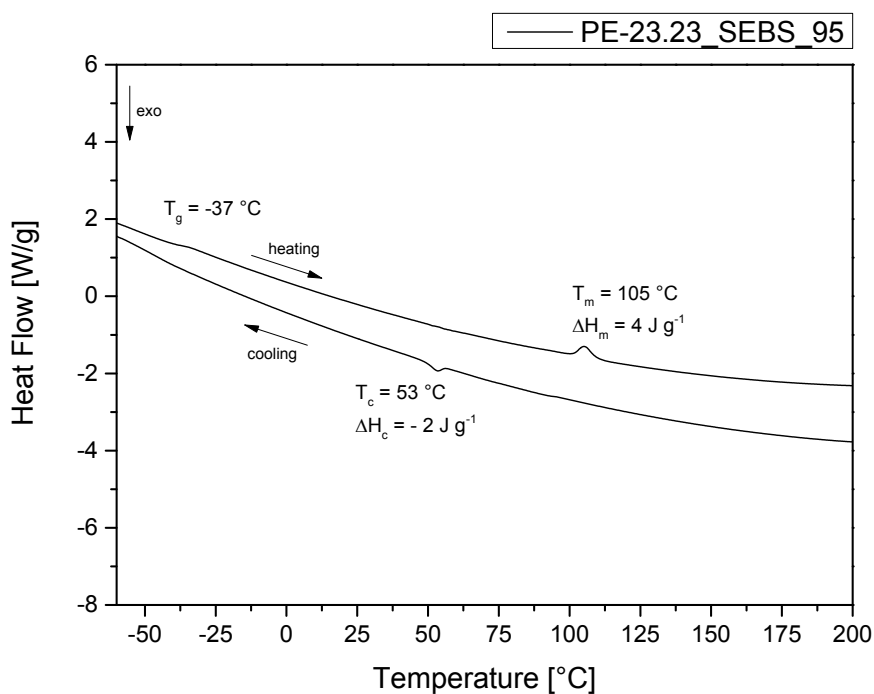


Figure S49: DSC analysis (15 K min^{-1} heating and cooling rate, respectively; data reported are from second heating cycles) of 5 wt. % PE-23.23 in Kraton G1643 MS (SEBS).

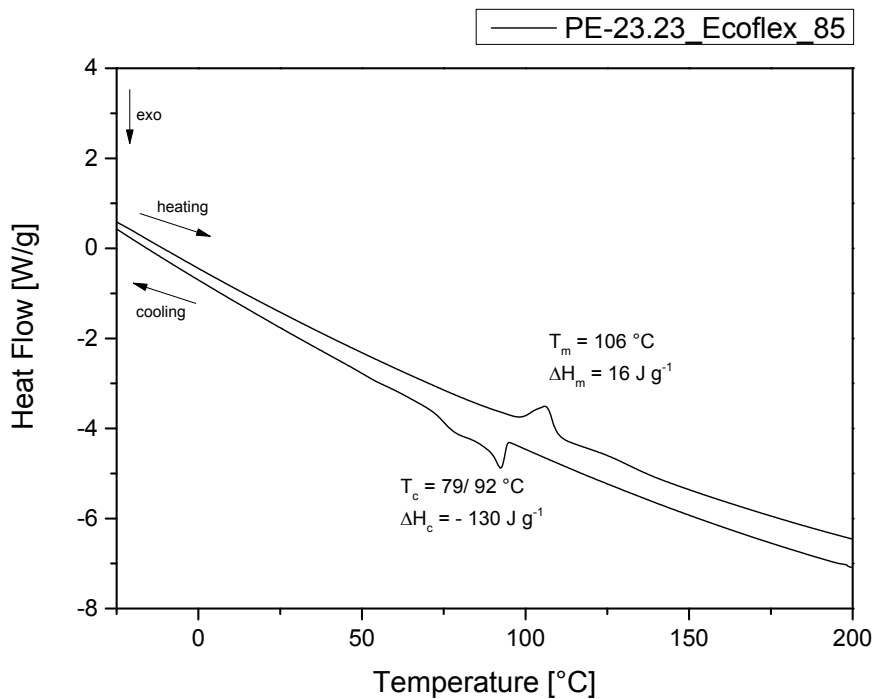


Figure S50: DSC analysis (15 K min⁻¹ heating and cooling rate, respectively; data reported are from second heating cycles) of 15 wt. % PE-23.23 in Ecoflex F Blend C1200.

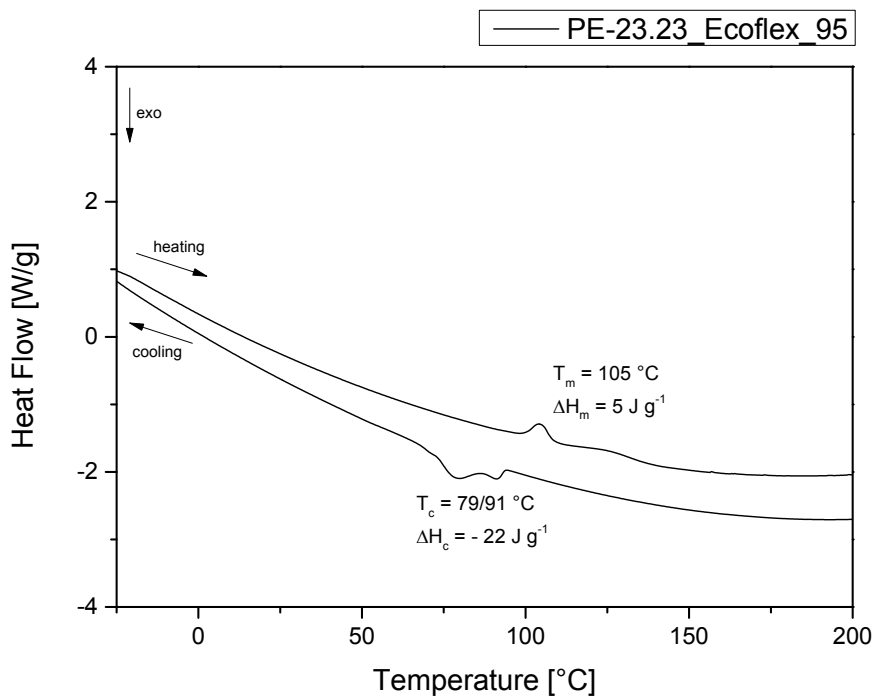


Figure S51: DSC analysis (15 K min⁻¹ heating and cooling rate, respectively; data reported are from second heating cycles) of 5 wt. % PE-23.23 in Ecoflex F Blend C1200.

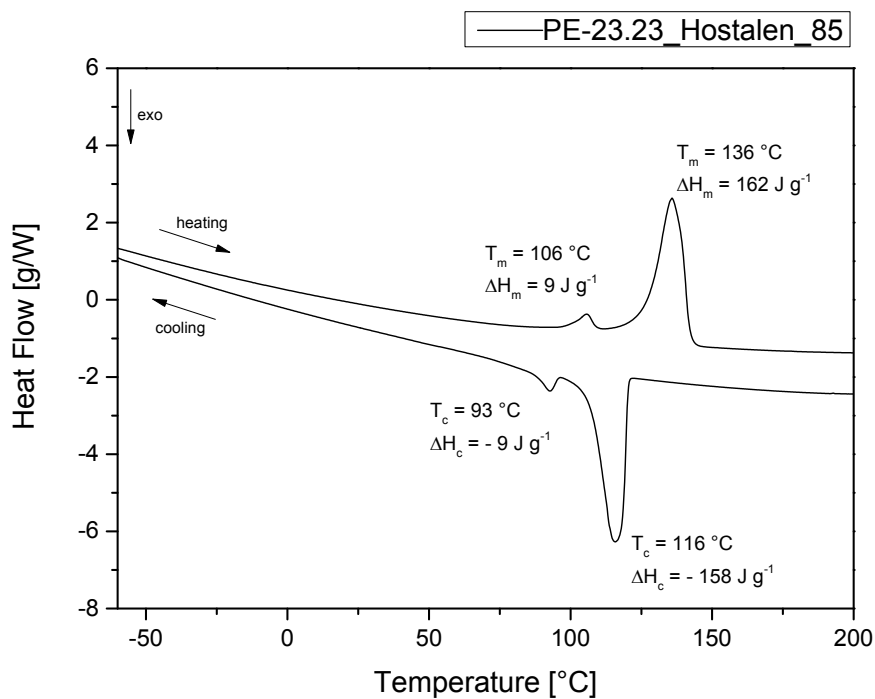


Figure S52: DSC analysis (15 K min^{-1} heating and cooling rate, respectively; data reported are from second heating cycles) of 15 wt. % PE-23.23 in Hostalen GC 7260 (HDPE).

SEM images of the polymer compounds

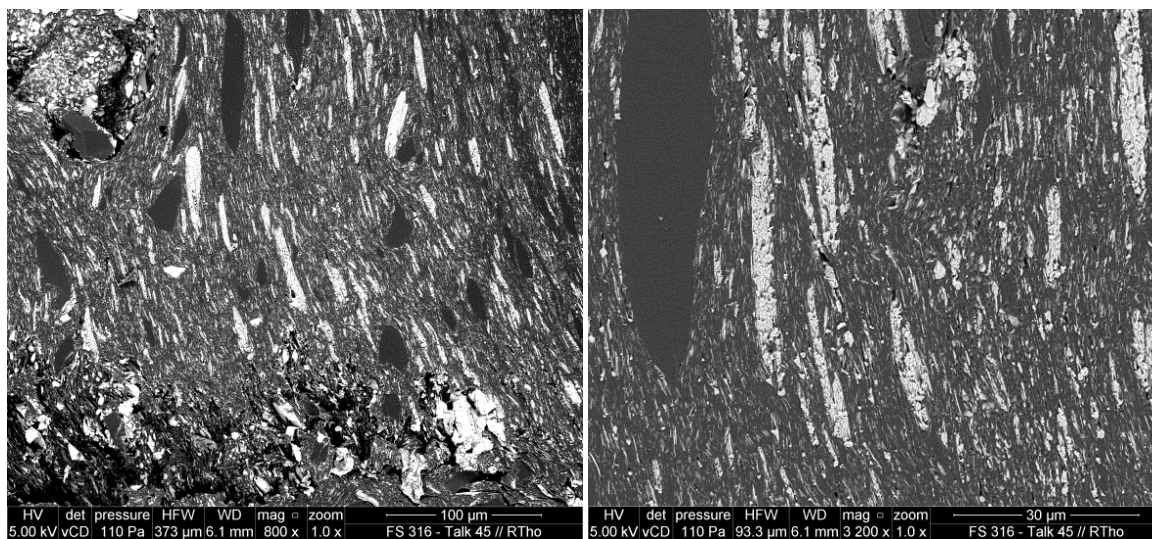


Figure S53: SEM images of PE-19.19 filled with 45 wt.% talc.

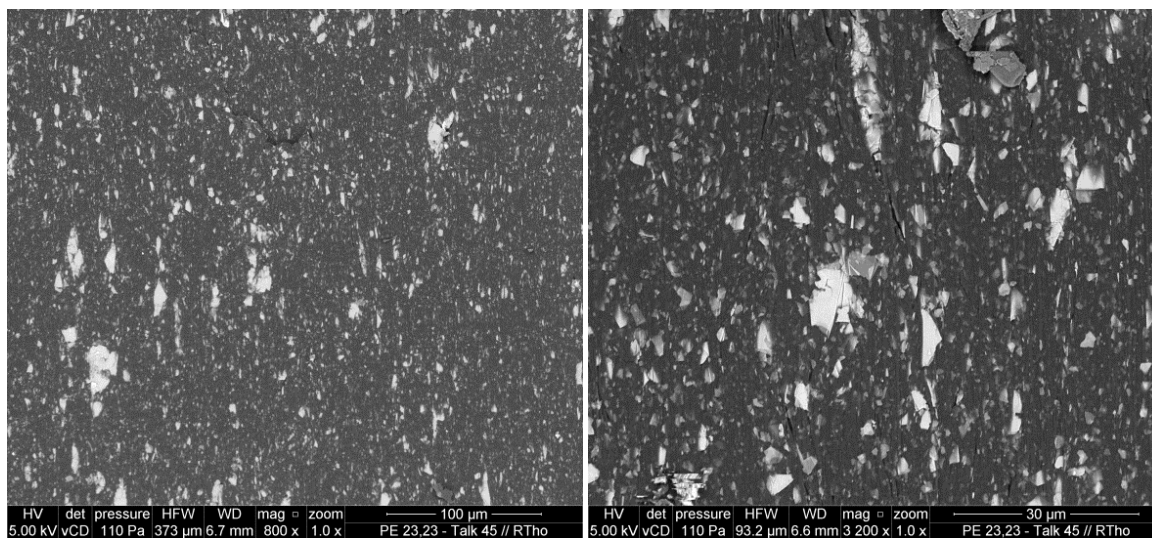


Figure S54: SEM images of PE-23.23 filled with 45 wt.% talc.

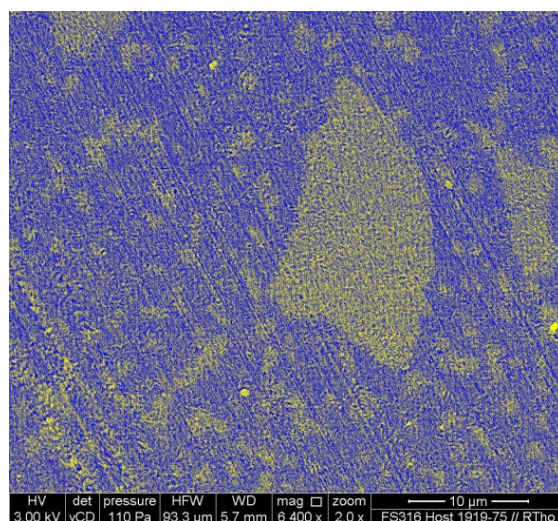


Figure S55: SEM images of 25 wt. % PE-19.19 in Hostalen GC 7260 (HDPE).

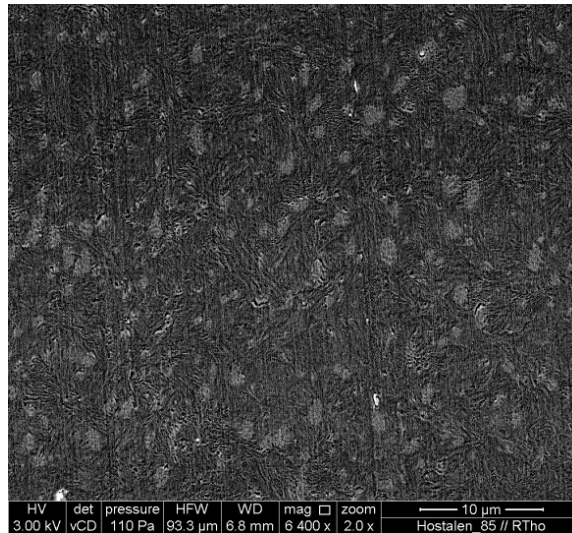


Figure S56: SEM images of 15 wt. % PE-23.23 in Hostalen GC 7260 (HDPE).

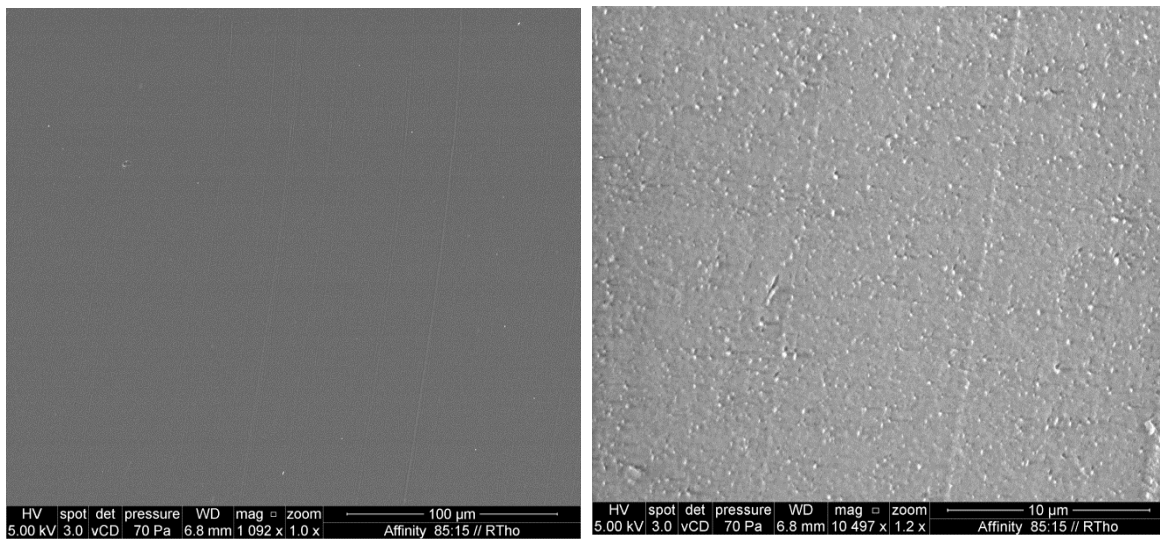


Figure S57: SEM images of 15 wt. % PE-23.23 in Affinity 8200G (LLDPE).

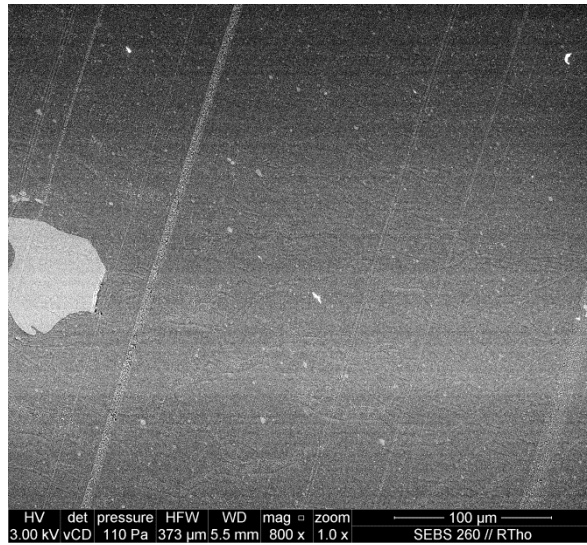


Figure S58: SEM images of 15 wt. % PE-23.23 in Kraton G1643 MS (SEBS).

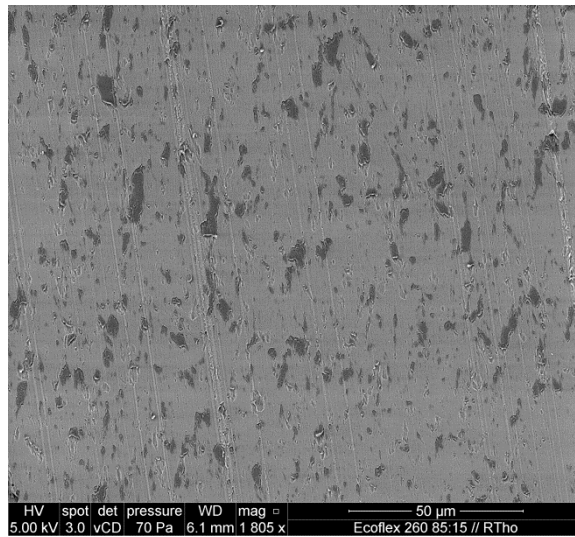


Figure S59: SEM images of 15 wt. % PE-23.23 in Ecoflex F Blend C1200.

¹ J. R. Prakash. *J. Rheol.*, 2002, **46**, 1353.